Reliability Engineering and System Safety 265 (2026) 111489

Contents lists available at ScienceDirect

Reliability Engineering and System Safety

journal homepage: www.elsevier.com/locate/ress

Resilience assessment: Insights from port community structures across the global container shipping network

Xuri Xin, Zaili Yang *

Liverpool Logistics, Offshore and Marine (LOOM) Research Institute, Liverpool John Moores University, Liverpool, United Kingdom

A R T I C L E I N F O

Keywords:
Resilience assessment
Global container shipping network
Directed-weighted network
Community structure
Port disruption

A B S T R A C T

Assessing resilience of the Global Container Shipping Network (GCSN) is crucial for bolstering its preparedness against various disruptions. Despite the growing prominence of regionalization within the GCSN, the precise impact mechanism of this trend on network resilience remains largely unexplored. To address this gap, this study introduces a new methodology for assessing the GCSN resilience from a community-based perspective. Initially, a directed-weighted GCSN is constructed utilizing global container shipping service data, facilitating the fine-grained identification of overlapping community structures through Symmetric Nonnegative Matrix Factorization (SNMF). Subsequently, six innovative community-based resilience metrics are devised, accounting for network directionality and link weight, thereby enabling a reliable assessment of community networks' capacity to maintain both connection efficiency and extent across different community dimensions. Various disruption scenarios, incorporating different disruption dimensions, attacked port characteristics, and disruption types, are designed to thoroughly evaluate community resilience. Experimental results reveal that 10 identified communities maintain strong intra-community connections but are highly vulnerable to disruptions at intra-community hub ports. These disruptions potentially lead to significant resilience degradation and network collapse, especially under targeted cumulative attacks. Consequently, this research contributes new insights into the mechanisms of community-based shipping network resilience and informs strategic decision-making to mitigate various disruption risks.

1. Introduction

The Global Container Shipping Network (GCSN), being a critical component of the international transportation system, plays an indispensable role in facilitating international trade and economic activities. However, the growing frequency of both natural and man-made turbulences exposes the GCSN to a range of potential risks. These risks encompass local-level disruptions (e.g., typhoons, labor strikes, terrorism, canal blockage, and accidents), regional-level challenges (e.g., trade wars and geopolitical tensions), and even global-level shocks (e.g., global pandemic and conflicts) [1]. These emerging risks are considered non-classical due to their devastating, abnormal, and unpredictable nature, often causing network disruptions that hinder the smooth operation of shipping trade, resulting in economic losses and even supply chain collapses. Illustrative instances include the Suez Canal obstruction leaving vast amounts of cargo stranded [2], stringent anti-COVID-19 measures causing congestion at numerous ports in China [3], and the Russia-Ukraine conflict leading to interruptions in the associated supply chains [4]. Given the expanding coverage of shipping services, rendering the network more complex and susceptible, understanding the impact of various disruptions on the GCSN compared to normal circumstances is imperative for better preparation and response to potential risks.

Resilience stands as a crucial measure for evaluating a system's capacity to maintain functionality during disruptions and to rebound to its previous performance level thereafter [5,6]. Through a comprehensive assessment of resilience, stakeholders can promptly identify potential risks and understand the impacts of disruptions on a system. This process is instrumental in pinpointing bottlenecks and critical components within the system, while also facilitating the formulation of strategies to

Abbreviations: BC, Betweenness Centrality; CC, Closeness Centrality; DC, Degree Centrality; GCSN, Global Container Shipping Network; LCC, Largest Connected Component; NMF, Nonnegative Matrix Factorization; *Ncut*, Normalized Cut; SNMF, Symmetric Nonnegative Matrix Factorization; UED, Unconventional Emergency Disruptions.

* Corresponding author.
E-mail address: Z.Yang@ljmu.ac.uk (Z. Yang).

https://doi.org/10.1016/j.ress.2025.111489
Received 14 September 2024; Received in revised form 12 June 2025; Accepted 21 July 2025
Available online 22 July 2025

enhance system resilience to some degree. Within this context, numerous studies have delved into resilience assessment across diverse maritime transportation investigations, highlighting its role in understanding network risks and supporting system recovery to maintain uninterrupted shipping operations [7–12,61]. As a result, conducting systematic resilience assessment for the GCSN under various disruptions emerges as an especially critical pursuit for both governments and other relevant stakeholders, such as port authorities and shipping companies, to enhance readiness for potential risks in an era marked by high uncertainties and continuous turbulence.

Nonetheless, the current research primarily focuses on examining the resilience of the GCSN from a global perspective [13–15]. However, the structure of the GCSN mirrors the dual trends of globalization and regionalization, characterized by more intensive intra-regional connections and a few essential routes linking different regions. Particularly in recent years, the COVID-19 pandemic has markedly amplified anti-globalization sentiments and escalated geopolitical conflicts, resulting in a surge in short-distance trade and increased friction in long-distance trade [9,16]. Consequently, the GCSN displays significant community structure characteristics, where ports within the same community exhibit denser connections while those between communities have relatively sparse connections. By identifying such communities, one can reveal nuanced intra- and inter-regional or functional linkages within the network. Accurately detecting densely connected communities helps clarify capacity allocation, the roles of key ports, and regional trade-corridor patterns, while pinpointing sparsely connected inter-community routes, often dependent on a few hub ports, offers clearer insights into vulnerabilities and the risk of disruption spillovers. Compared to solely examining the network at the global level, assessing resilience through a community-based lens helps uncover failure modes of critical nodes and reveals how inter-community dependencies influence overall network stability. Moreover, community-level analysis enables more targeted interventions tailored to specific community scales, hierarchies, and functions. Thus, incorporating community detection into resilience assessments of the GCSN fosters a deeper understanding of network structure and lays a solid foundation for enhancing the sustainability of the shipping network and its capacity to withstand multifaceted shocks.

Although previous studies have examined the community structures of the global shipping network [14,16,17], they exhibit one or more of the following limitations: overlooking overlapping community characteristics, oversimplifying network directionality and weight characteristics, and facing limitations in detecting community structures of varying sizes. Additionally, resilience assessment for the GCSN from a regionalization or community-based perspective remains largely unexplored, despite its crucial importance in comprehending the effects of various disruptions on regional shipping networks and aiding stakeholders in devising precise, sustainable interventions tailored to different community scales. To date, there has been scant comprehensive work on the community-based resilience characteristics of the GCSN, which necessitates simultaneously incorporating advanced community detection algorithms, developing effective port community-based resilience metrics, and designing a systematic scenario-based resilience evaluation framework that accommodates various disruption scenarios. Hence, formulating a comprehensive community-based resilience assessment approach for the GCSN that addresses these limitations represents a valuable yet challenging undertaking and illustrates the primary novelties of this work.

This study aims to develop a new methodology for assessing the resilience of the GCSN from a community-based perspective. Specifically, it focuses on the initial stages of resilience, namely a system's ability to maintain its functions amidst disruptions. This focus is crucial because the time required for recovery is exceedingly difficult to determine, and recovery is often impractical for maritime transportation networks in the short term, especially when faced with Unconventional Emergency Disruptions (UED) [1]. To fulfill this goal, a directed-weighted GCSN is first established using worldwide container shipping service data from 2022. Subsequently, an advanced graph clustering technique known as Symmetric Nonnegative Matrix Factorization (SNMF) is employed to identify fine-grained overlapping community structures within the GCSN. Meanwhile, the unique hub functions of each port, including provincial, gateway, and connector hubs, are captured in terms of the connection patterns within the GCSN's community configurations. Following this, six innovative quantitative metrics are introduced to quantify the resilience of port community in maintaining both connection efficiency and extent when faced with various disruptions. Building on this, a scenario-based resilience evaluation framework is developed to systematically examine community-level responses to different disruption types. Together, these components offer a holistic approach to assessing community resilience within the GCSN, enhancing understanding of network robustness, guiding disruption mitigation, and shaping shipping services.

The remainder of this paper is structured as follows: Section 2 provides a review of pertinent literature on network modeling, community detection, and resilience assessment within shipping networks, elucidating research gaps and novel contributions. Section 3 details the newly developed methodology, including the construction of the GCSN, port community structure analysis, resilience measurement metric development, and establishment of a scenario-based resilience assessment framework. Section 4 performs an application analysis to extract insights and implications. Finally, Section 5 summarizes the conclusions and proposes avenues for future research.

2. Literature review

This study covers two main areas of literature. Firstly, it investigates research on shipping network modeling and methods for detecting port communities. Secondly, it focuses on studies related to the resilience assessment of shipping networks. These reviews aid in identifying research gaps and making new contributions.

2.1. Shipping network modeling

A robust shipping network model serves as the cornerstone for analyzing network characteristics. Extensive research effort has been directed towards exploring various aspects within constructed shipping networks. These primary aspects include examining network topological features [15,16,18,62], detecting community structures [14,17], assessing node centrality levels [19], analyzing core-periphery structures [20], and investigating network resilience and vulnerability [1,21–24]. Additionally, researchers have delved into how shipping networks evolve in response to disruptions, such as the COVID-19 pandemic [25,26] and the emergence of the Arctic route [27]. Generally, shipping networks can be created using two main data sources: ship movement trajectory data and shipping service route data [14,16,28,29,63]. The former comprises lists of visited ports extracted from extensive volumes of trajectory data, while the latter records the predetermined ports visited along shipping routes. Unlike ship movement trajectory data, service route data exclusively focuses on details directly pertinent to cargo transport, excluding irrelevant information and eliminating the need for additional processing tasks such as trajectory cleaning and reconstruction. Consequently, this study leverages shipping service data to establish a directed-weighted GCSN, accounting for the disparate distribution of maritime cargo trades and the asymmetric structure of pendulum services, thereby offering a more accurate representation of real-world network dynamics.

Community structure detection, as a prominent field in complex network analysis, is critical for comprehending the complex patterns and functional dynamics of the GCSN from a regionalization perspective. Recent research [14,16] highlighted that the GCSN mirrors a dual trend of globalization and regionalization, characterized by stronger intra-regional connections contrasted with sparse inter-regional links.

This observation aligns closely with the inherent community structures of complex networks. Thus, leveraging insights from community detection methods, the GCSN can be partitioned into numerous port communities that exhibit high intra-connectivity but low inter-connectivity. Numerous studies have explored the community structures within the GCSN, employing various divisive algorithms such as Spectrum-based algorithms [30], the Infomap algorithm [16,31,32], and Louvain-based Modularity optimization techniques [17,33], demonstrating their effectiveness in identifying non-overlapping communities. However, challenges arise, particularly concerning ports located at regional boundaries or strategic points like straits and canals, where shipping routes are evenly distributed among different communities. Evidently, the GCSN displays pronounced overlapping community characteristics, with certain ports serving as bridges across multiple communities. In response to this, Bai et al. (2023) [14] applied the Clique Percolation method to capture realistic overlapping community structures within the global shipping network. Nevertheless, this approach faces limitations, including high sensitivity to k-clique selection, the necessity to eliminate weak links to adapt to weighted networks, and constraints in detecting community structures of varying sizes, leading to low resolution. Consequently, there is an urgent need for an efficient community detection algorithm capable of accurately characterizing fine-grained overlapping community structures within the GCSN.

SNMF, as a sophisticated technique for community detection, excels in the analysis of complex networks. Its strengths are evident in several key areas: 1) It offers exceptional versatility, enabling the adaptation of varied adjacency measures that accurately reflect the structural nuances of datasets; 2) It outperforms other clustering algorithms, achieving higher accuracy and interpretability in graph-based partitioning tasks; 3) Its inherent soft clustering mechanism naturally facilitates the detection of overlapping communities by allowing each node to belong to multiple communities simultaneously; and 4) It provides control over the degree of overlap among communities through precise tuning of membership parameters, ensuring an optimal balance between community overlap and distinctiveness [34,35]. These features have propelled SNMF into many successful applications across various research domains, such as community detection in node-social networks [36], road traffic network partitioning [37,38], and ship traffic partitioning [39–41]. Table 1 presents a comparative overview of current port community detection methods, including SNMF. As a result, this study presents a pioneering application of SNMF for identifying fine-grained overlapping community structures within the GCSN, thus supporting subsequent network resilience analyses from a regional community perspective.

2.2. Resilience assessment of shipping network

The concept of resilience varies across different disciplines, yet it is generally defined as a system's capacity to resist, absorb, adapt to, and recover from adverse disruptions [42–44]. Additionally, various other concepts such as vulnerability, robustness, reliability, and flexibility are commonly utilized to assess system performance when confronted with potential internal and external disruptions. Resilience distinguishes itself from these concepts by offering a broader perspective, emphasizing the system's ability to 'absorb and persist' against changes arising from both the supply and demand sides. The subsequent analysis is centered on examining the application of resilience alongside other relevant concepts within shipping networks.

Numerous researchers have led pioneering efforts to quantify, analyze, and enhance the resilience of shipping networks using innovative concepts, definitions, and methodologies. For instance, Dui et al. (2021) [45] introduced the concept of "residual resilience", which evaluates the remaining value relative to the loss incurred during the recovery phase. They subsequently utilized an optimization model to prioritize port repair sequences following disruptions, aiming to maximize residual resilience. Qin et al. (2023) [46] proposed a three-dimensional econometric model that incorporates port structure, function, and location to assess port-node resilience in the face of external shocks. This model accommodates the intricate linkages and attributes of port nodes within the shipping network. Asadabadi and Miller-Hooks (2020) [47] devised a series of stochastic, bi-level, game-theoretic optimization models to evaluate and enhance the resilience of the global port network. Their methodology accounts for uncertainties in traversal times and port throughput capacities, enabling a comprehensive resilience evaluation of their impact on served demand, throughput, and shipping costs. Among these studies, one of the most prevalent approaches to assessing shipping network resilience is based on complex network theory, which examines the impact of various disruptions on the topological characteristics of the shipping networks. Briefly speaking, an effective assessment of shipping network resilience requires addressing two crucial issues: firstly, selecting and constructing effective metrics to measure resilience, and secondly, designing disruption scenarios to simulate the impact on network performance.

Regarding the metrics adopted to measure resilience, various network-based metrics such as connected component size, clustering coefficient, Betweenness Centrality (BC), Degree Centrality (DC), Closeness Centrality (CC), network efficiency, Largest Connected Component (LCC), and motif-based metrics have been utilized to evaluate shipping network performance under disruptive circumstances [15, 48–51]. These metrics primarily focus on analyzing the topological characteristics of the network and treat the shipping network as an undirected and unweighted system, thereby overlooking the influence of network directionality and link weight on network functionality. However, the shipping network is a directed-weighted network, where link weights reflect the cargo service capability of shipping routes between two ports and directed links disclose the sequence of departure for shipping routes between them [16]. In light of this, extensions and refinements of network metrics have emerged to leverage this valuable information within shipping networks, aiming to more accurately characterize network features. For instance, Bai et al. (2023) [14] employed a network disintegration method proposed by Zhou et al. (2021) [52] to enable network-based metrics to accommodate weighted networks. Liu et al. (2022) [19] introduced service-based DC, CC, and BC weighted by connection intensity (i.e., service capacity) of links to measure a port's connectivity level. Additionally, novel metrics such as the average of after-before degree ratios and the average of after-before closeness ratios [1] were proposed to reflect the "overall connection level" of the "remaining network" after disruptions. Despite these advancements, the aforementioned metrics exhibit two significant limitations when supporting community-based resilience measurement within the GCSN. Firstly, most existing metrics capture only singular aspects of the influence of network directionality and link weight on network operational performance, or they disregard both factors altogether.

Table 1
Comparative overview of port community detection methods.

Method	Support weighted networks	Support overlapping communities	Interpretability	Ease of integrating external information	Cluster count control
Spectral [30]	Yes	No	Moderate	Yes	Yes
Louvain [17,33]	Yes	No	Moderate	Yes	No
Infomap [16,31]	Yes	No	Moderate	Yes	No
Clique [14]	Partial	Yes	Moderate	Yes	Partial
SNMF	Yes	Yes	Good	Yes	Yes

Secondly, these metrics primarily concentrate on measuring the overall performance of the shipping networks, neglecting the community structure characteristics within them. Therefore, the development of advanced metrics that incorporate both network directionality and link weight from a regional community analysis perspective is essential for effectively measuring port community-based resilience.

Disruption simulation scenarios can be tailored to disrupt both nodes and links within a network. These disruptions are typically categorized as either random or deliberate. Random disruptions entail the arbitrary selection of nodes or links for attack, whereas deliberate disruptions typically follow a specific sequence, attacking nodes or links in terms of their importance. In node-based disruptions, researchers have employed diverse deliberate scenarios. Liu et al. (2018) [49] utilized the local efficiency clustering coefficient and global network efficiency to determine port attack sequences. Bai et al. (2023) [14] assessed node importance using weighted BC, DC, and CC. Liu et al. (2023) [1] explored three potential attack strategies: prioritizing nodes based on throughput volumes, centrality roles, or geographical locations. Noteworthy, the closure of specific shipping routes between ports is as common as individual port closures, such as through the implementation of entry restriction policies. Consequently, research has also examined the impact of deliberate link-based disruptions on shipping networks. For instance, Viljoen and Joubert (2016) [48] analyzed shipping network robustness and flexibility by iteratively removing links based on betweenness-based and salience-based scenarios. Calatayud et al. (2017) [53] examined a country's liner shipping service vulnerability by eliminating both inbound and outbound links. Additionally, some studies [13,14,50] have proposed cascading simulation models incorporating traffic flow redistribution rules to understand global shipping network resilience and vulnerability under cascading failures. Despite their valuable insights into disruption impact, the influence of regionalization on disruption scenario design is currently overlooked to a large extent. Additionally, an integrated scenario-based resilience evaluation framework, which simultaneously accommodates different disruption dimensions, attacked port characteristics, and disruption types from a community-based analysis perspective, remains unexplored, despite its crucial role in facilitating a holistic understanding of community resilience mechanisms amidst varied turbulences. Hence, it is imperative and promising to devise a novel framework capable of collectively analyzing community-based resilience across multiple disruption scenarios.

2.3. Research contributions

After a thorough literature review and gap identification, it is evident that there is a pressing need for substantial efforts to develop a holistic community-based resilience assessment methodology tailored to the GCSN. This methodology should possess the capability to extract fine-grained overlapping port community structures, devise advanced community-based resilience measurement metrics suited to directed-weighted networks, and formulate a series of disruption scenarios to holistically assess their impact. This study represents a pioneering effort in examining community-based resilience, addressing the aforementioned challenges to enhance understanding of the effects of various disruptions on regional service networks. Specifically, the key contributions of this study are outlined as follows:

1 A pioneering holistic methodology for assessing port community-based resilience is proposed, integrating advanced community detection techniques, novel quantitative resilience metrics, and a diverse range of disruption scenarios.
2 A graph-based clustering technique, SNMF, combined with a Newton-like algorithm, is employed to detect communities within the GCSN. This approach enables the fine-grained identification of hierarchical community structures without resolution limits and supports the discovery of overlapping communities through its inherent soft clustering capability.
3 Six novel metrics are developed to assess port community-based resilience, capturing the ability to maintain connection efficiency and extent under various disruptions. They provide comprehensive insights into intra-, inter-, and overall community connectivity, while accounting for network directionality and link weights in the GCSN.
4 A systematic scenario-based resilience evaluation framework is designed to enable a holistic assessment of community resilience within the GCSN. The scenarios in the framework span individual and cumulative disruptions, partial and complete failures, and account for affected ports' community membership, functional roles, and topological features.

3. Methodology: port community-based resilience assessment

This section outlines the proposed methodology for community-based resilience assessment, comprising four functional modules (see Fig. 1): 1) GCSN construction; 2) port community structure examination; 3) development of community-based resilience measures; and 4) formulation of a scenario-based resilience evaluation framework. The GCSN construction establishes the foundational element for the port community structure examination. Subsequently, leveraging the identified port community structures and proposed community-based resilience measures, a holistic framework for community-based resilience assessment is developed, accommodating diverse disruption scenarios. Technical details of each module are elaborated in the subsequent subsections.

3.1. GCSN construction

To investigate the resilience of the GCSN from a regionalization perspective, a weighted-directed GCSN, denoted as $G(V_N, E_L)$, should be established first. Here, nodes $V_N = \{v_1, v_2, \ldots, v_N\}$ represent ports, and links $E_L = \{e_{ij} | v_i \in V_N \cap v_j \in V_N\}$ represent connection routes between ports, as defined by the movement of container ships. Acquiring attributes of the GCSN involves leveraging container shipping service route data to gather crucial voyage details, such as the originating and departure ports, cargo service capacity, and duration of the journey. By utilizing this service route data, the weight (i.e., cargo service capacity) of a given link is determined by aggregating the deployed cargo service capacity of all container ships traversing the link. The directionality of each link is established by the sequence of predetermined ports along the shipping routes. Through this methodical process, a weighted-directed network is systematically constructed. The shipping service data collected is detailed in Section 4.1.

3.2. Port community structure examination

Port community structure examination entails two important components: one is the selection of graph-based community detection algorithms, which concerns the approaches and techniques adopted to effectively identify the fine-grained overlapping community structures within the GCSN; the other is the analysis of each port's functions within

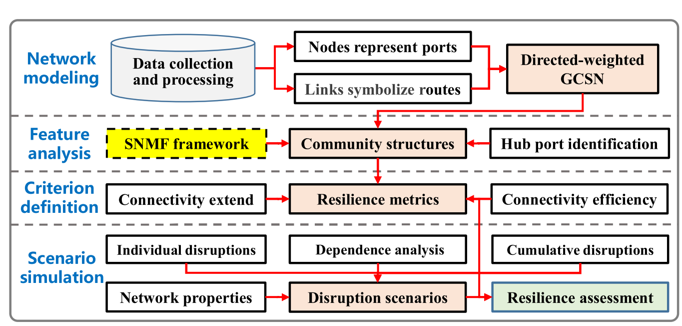

Fig. 1. Methodology diagram.

each identified community, which necessitates the comprehensive identification of hub ports with specific connection patterns.

3.2.1. Port community detection

Port community detection can be viewed from a graph-cut perspective. Given the constructed $G(V_N, E_L)$, port communities represent the subgraphs of G, characterized by dense intra-cluster connections among nodes and sparse inter-cluster connections. Assuming that G is comprised of k port communities, the community set is defined as $C = \{C_p | C_p \neq \varnothing, 1 \leq p \leq k\}$. To perform community partitioning, this study employs SNMF due to its numerous advantages, including flexibility, generality, and interpretability, especially in detecting overlapping communities within network-based scenarios (see Section 2.1). It is important to note that the SNMF model operates effectively with symmetric adjacency matrices. However, the adjacency matrix $A = [A_{ij}]_{N \times N}$ derived from G is non-symmetric due to the inclusion of cargo transportation directionality. Therefore, the nonnegative symmetric adjacency matrix W utilized for SNMF can be initially obtained as $W = (A + A^T)/2$, where A^T represents the transpose of A.

The fundamental idea of SNMF is to approximate W with a symmetric nonnegative low-rank matrix H. This process minimizes connections between clusters while maximizing connections within a cluster. The achieved objective in theory is mathematically equivalent to a trace maximization formulation, as outlined below:

$$
\begin{aligned}
&\max_{H \geq 0, H^T H = I} \boldsymbol{Tr}\left(H^T W H\right) \Leftrightarrow \\
\min_{H \geq 0, H^T H = I} &\boldsymbol{Tr}\left(W^T W\right) - 2\boldsymbol{Tr}\left(H^T W H\right) + \boldsymbol{Tr}\left(H^T H\right) \Leftrightarrow \\
&\min_{H \geq 0, H^T H = I} \| W - HH^T \|_F^2
\end{aligned}
\tag{1}
$$

where $W \in \mathbb{R}_+^{N \times N}$, and $H \in \mathbb{R}_+^{N \times k}$, subject to $H^T H = I$ and $H \geq 0$. However, achieving the optimal solution to the graph-cut optimization objective presents a challenge due to the NP-hard nature of the problem, arising from the imposition of two constraints on H. Hence, to make the formulation tractable, SNMF relaxes the orthogonality constraint. Previous research [54] has underscored the importance of the nonnegativity constraint on H over the orthogonality constraint. Meanwhile, maintaining the nonnegativity constraint through SNMF leads to a near-orthogonality approximation of the columns in matrix H. This characteristic positions SNMF favorably and holds promise for effectively tackling the challenge of graph-based community detection.

To produce port communities with a balanced size distribution, the commonly employed objective function known as Normalized Cut (*Ncut*) is utilized [38]. It aims to minimize the connection strength between different groups while maximizing the cohesion within groups, taking into account the weights of connections. This balanced approach ensures that cuts do not merely isolate a few points from the rest of the network; instead, they tend to form groups that are reasonably sized and tightly knit internally. The function is represented as follows:

$$
Ncut(C_1, C_2, \cdots, C_k) = \boldsymbol{Tr}\left(H^T D^{-\frac{1}{2}} L D^{-\frac{1}{2}} H\right) \tag{2}
$$

where D represents the diagonal matrix with $D_{ii} = \sum_{j=1}^{N} W_{ij}$, and L denotes the Laplacian matrix of W. Minimizing *Ncut* can be equivalently achieved by substituting W in Eq. (1) with a normalized adjacency matrix, denoted as $\widetilde{W} = D^{-1/2} W D^{-1/2}$. Consequently, with the similarity matrix $\widetilde{W}$ and the desired number of communities k determined, the SNMF model for port community detection can be expressed in the following manner:

$$
\min_{H \geq 0} L(\widetilde{W}, k) = \| \widetilde{W} - HH^T \|^2 \tag{3}
$$

To address the minimization problem outlined in Eq. (3), the Newton-like algorithm is employed for its efficacy in handling small-scale problems (e.g., when the number of objects to be clustered does not exceed 3000) and its capability to yield superior clustering outcomes [35]. However, the optimization process of the Newton-like algorithm is sensitive to the initialization of H, making it unrealistic to expect the algorithm to converge to the global minimum in a single execution. Therefore, the Newton-like algorithm is executed multiple times with randomly sampled initial H to obtain a solution that is either a global minimum or at least guarantees a near-global minimum.

After obtaining the optimal matrix H, each row can be interpreted as the membership of ports belonging to different communities. Hence, the communities can be easily inferred based on H, regardless of whether considering the overlapping of communities. For detecting overlapping communities, a membership threshold φ must be established. Then, if the normalized $H_{ip} > \varphi$, port i is assigned to the pth community. This approach enables port i to be assigned to multiple communities. By adjusting the parameter φ, one can control the degree of overlap among communities. Fig. 2 illustrates the general process of SNMF-based overlapping port community detection.

For the practical implementation of SNMF in port community detection, two input parameters, k and φ, should be identified in advance, which are crucial for optimal community partition performance. Regarding the value of k, the hand-elbow method is adopted due to its simplicity and reliability. *Ncut* is used as the evaluation metric, given its comprehensive consideration of both network topology characteristics and network connection weight, thus yielding more precise and effective detection results compared to other metrics like modularity and modularity density [55]. When k is less than the actual community number, increasing k greatly enhances the aggregation degree within each community, resulting in a marginal rise in *Ncut*. However, as k approaches the true community number, the aggregation degree within each community diminishes with an increase in k, causing a significant increase in *Ncut*. The relationship between *Ncut* and k typically exhibits an elbow-shaped curve, with the value of k at the elbow point indicating the actual number of communities.

As for the value of φ, it depends on the application demand for balancing overlap and separation between communities. A lower φ allows ports to belong to multiple communities simultaneously, while a higher φ ensures distinct boundaries between different communities. This study determines the accurate φ value manually based on the number of overlapping ports and the number of ports belonging to at least one community, as elaborated in detail in Section 4.2.

3.2.2. Hub port identification

Utilizing the identified community structures within the GCSN, three distinct types of hub ports, namely provincial, gateway, and connector hubs, are discerned based on both intra-community and inter-community connection patterns, as indicated by previous studies [14, 17]. These hub ports play a pivotal role in facilitating resilience analysis from a port community perspective. Acknowledging the GCSN's nature as a directed network with unbalanced cargo transportation, an extension is implemented to integrate directional information within the links, thereby enhancing the accuracy of measuring port centrality levels when identifying hub ports.

Provincial hubs are characterized by ports that exhibit strong connections with other ports within their respective community. The intra-community degree of a port is outlined as follows:

$$
Z_i = \left. \frac{z_{ip} - \overline{z}_p}{\sigma_{z_T}} \right|_{i=1:N} \tag{4}
$$

where port i pertains to the pth community, z_{ip} represents the cumulative count of inbound and outbound links between port i and other ports within the pth community. $\overline{z}_p$ and σ_{z_T} represent the mean and standard deviation of z_{ip} within the pth community, respectively. Ports with Z_i values equal to or exceeding 1.5 are designated as provincial hubs.

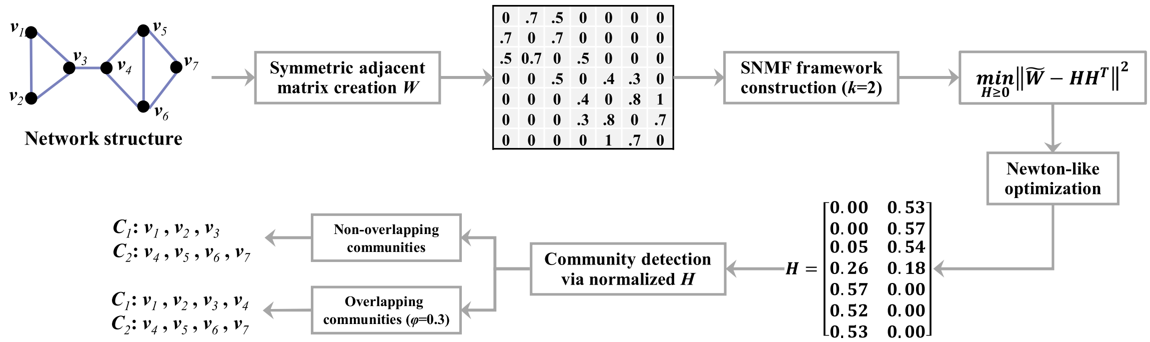

Fig. 2. Illustration of port community detection process using SNMF.

Gateway hubs are characterized by ports that boast strong connections with ports outside their community. The outside-community degree of a port is outlined as follows:

$$B_i = \left. \frac{b_{ip} - \bar{b}_p}{\sigma_{b_p}} \right|_{i=1:N} \tag{5}$$

where port i pertains to the pth community, b_{ip} signifies the cumulative count of inbound and outbound links between port i and other ports beyond the pth community. $\bar{b}_p$ and σ_{b_p} represent the mean and standard deviation of b_{ip} within the pth community, respectively. Ports with B_i values equal to or exceeding 1.5 are designated as Gateway hubs.

Connector hubs are characterized by ports with links distributed evenly among multiple communities. The participation coefficient is employed to assess the uniform distribution of a port's links among different communities, defined as follows:

$$P_i = 1 - \left. \sum_{p=1}^{k} \frac{z_{ip}}{z_i} \right|_{i=1:N} \tag{6}$$

where z_i represents the total degree of port i, comprising both inbound and outbound connections, z_{ip} signifies the count of inbound and outbound links of port i to other nodes within the pth community. k denotes the total number of communities within the network. A P_i value of 0 indicates that all neighbors of a given port reside within its own community, whereas a P_i value approaching 1 signifies a uniform distribution of neighbors across all communities. Ports with P_i values equal to or greater than 0.7 are recognized as connector hubs.

3.3. Port community-based resilience measures

To evaluate the resilience of communities within the GCSN against diverse disruptions, this study introduces six novel metrics as quantitative measures to evaluate each community's capacity for maintaining network connectivity amidst disruptions at the disruption stage. These metrics focus on two pivotal aspects: "connection efficiency", which reflects the ability of ports to rapidly transport goods over the shortest possible journey or timeframe, emphasizing the importance of timeliness in maritime logistics [14]; and "connection extent", which assesses whether a port maintains viable direct or indirect pathways to other ports, thereby showcasing the reachability of the network [56]. By integrating these measurements and applying them across three levels, within individual communities, between different communities, and across the overall community network, it aims to comprehensively capture the regional and overall changes in response to disruptions. It is important to note that these metrics not only measure port interactions through "shortest transit time" and "reachability" but also incorporate network directionality and capacity weight to more accurately reflect the actual operational differences in maritime routes and port operations. In subsequent simulations and case studies within this research, these six metrics are utilized to depict the change in community connectivity under various disruption scenarios. Detailed explanations follow below.

Regarding network connection efficiency, the reciprocal of the shortest path lengths between node pairs is commonly employed to evaluate information spreading with minimized time or cost [57]. This study, however, employs the inverse of the actual shortest travel time to measure the connection efficiency from one port to another within the GCSN, as it offers greater intuitiveness and accessibility compared to path lengths [14]. The definition is outlined as follows:

$$e_{ij} = \frac{1}{t_{ij,min}} \tag{7}$$

where $t_{ij,\min}$ denotes the actual directional shortest travel time from port i to j based on all available link services in the shipping network. A larger e_{ij} implies a higher transmission efficiency from port i to j.

In terms of network connection extent, one connection reachability metric is devised to reflect whether a port can transport goods to another port through various potential paths within the GCSN, as follows:

$$c_{ij} = \begin{cases} 1, & \text{if there is reachability from } i \text{ to } j \\ 0, & \text{if there is not reachability from } i \text{ to } j \end{cases} \tag{8}$$

where $c_{ij} = 1$ if there is reachability from port i to j through all potential links within the GCSN; otherwise, $c_{ij} = 0$. Evidently, if the GCSN exhibits a higher overall connection extent, finding paths from one port to reach another port becomes easier.

Building upon the network connection efficiency and network connection extent metrics defined above, six quantitative metrics for measuring the connectivity of port communities are further expanded and provided. Using network connection efficiency as an illustration, three efficiency metrics that comprehensively characterize the community efficiency functionality are defined as follows:

Definition 1. Intra-community efficiency measures the average connection efficiency between ports within the same community in the GCSN, as follows:

$$DE_{intra} = \frac{1}{|C_p| \cdot (|C_p| - 1)} \sum_{i \neq j \in C_p} e_{ij} \tag{9}$$

where $|C_p|$ represents the number of ports in the pth community.

Definition 2. Inter-community efficiency measures the average connection efficiency between one community and all other communities in the GCSN, as follows:

$$DE_{inter} = \left(\frac{1}{|C_p| \cdot |\overline{C}_p|} \sum_{i \in C_p, j \in \overline{C}_p} e_{ij} + e_{ji} \right) \Big/ 2 \tag{10}$$

where $|\overline{C}_p|$ represents the number of ports outside the pth community.

Definition 3. Overall community efficiency measures the average connection efficiency between each port within the community and all other ports both within and outside the community, as follows:

$$DE_{all} = \left(\frac{1}{|C_p| \cdot (N-1)} \sum_{i \in C_p, j \in C, i \neq j} e_{ij} + e_{ji} \right) \Big/ 2 \tag{11}$$

where N represents the number of ports in the GCSN. The above three metrics collectively assess community connection efficiency from different perspectives. Similarly, by substituting e_{ij} in Eqs. (9)-(11) with c_{ij}, the corresponding metrics DC_{inter}, DC_{intra}, DC_{all} can be readily derived to evaluate the connection extent of a community from multiple viewpoints.

The metrics mentioned above effectively consider the influence of directionality, given that the service paths' transit time or reachability can vary between transport directions i-j and j-i. However, they treat the GCSN as an unweighted network, overlooking the varying cargo service capacities (i.e., weights) across its links. Notably, links with higher service capacity exert a significantly greater influence on network connectivity. Therefore, to accommodate the network weight in the metrics, a network disintegration model proposed by Zhou et al. (2021) [52] is employed. This model breaks down the original weighted network into multiple unweighted subnetworks and calculates and integrates the metric values for each subnetwork. The effectiveness of this model has been demonstrated through comparisons with analyses conducted on unweighted networks in numerous studies [14,58]. The underlying principle of this model involves an iterative process. At each step, one unit of a link between all connected node pairs is removed from the original network. The removed links are then used to construct subnetworks, and this disintegration process continues until no links remain between any pairs of nodes. Once the subgraphs are obtained, the weighted-directed community connectivity quantification is achieved by calculating and integrating the aforementioned metric values of these decomposed subgraphs, as follows:

$$WDEC = DEC_1 + DEC_2 + \ldots + DEC_l \tag{12}$$

where l represents the number of subgraphs, and $DEC_q = \{DE_{inter,q}, DE_{intra,q}, DE_{all,q}, DC_{inter,q}, DC_{intra,q}, DC_{all,q}\}$ denotes the value of the directed community connectivity metrics associated with the qth subnetwork.

This study primarily focuses on how community networks remain well-connected when confronted with disruptions during the disruption stage. Thus, the metric representing the community network's resilience in maintaining its essential functions during disruptions is formulated as follows:

$$WDEC_A = \frac{WDEC_{post}}{WDEC_{pre}} \tag{13}$$

where $WDEC_A = \{WDE_{A,intra}, \mathrm{WDE}_{A,inter}, \mathrm{WDE}_{A,all}, WDC_{A,intra}, WDC_{A,inter}, WDC_{A,all}\}$ represents the normalized residual community connectivity against disruptions, and $WDEC_{pre}$ *and* $WDEC_{post}$ measure the community connectivity before and after a disruption. The values of $WDEC_A$ range from 0 to 1, with a higher value suggesting greater resilience against disruptions. For instance, a significant decline in "normalized residual intra-community connection efficiency" ($WDE_{A,intr}$) indicates that key ports or routes within a community have been compromised, leading to a substantial increase in average transport times within that community. This could result in stakeholders facing delays or incurring additional scheduling costs. Similarly, a sharp decrease in "normalized residual inter-community connection extent" ($WDC_{A,inte}$) suggests that a port community's capacity to connect and communicate with other communities has been severely weakened, hindering the smooth inter-community transport of goods from their original ports. In practical scenarios, these metrics can assist port managers and shipping companies in pinpointing vulnerabilities within community networks, offering essential evaluative support to strategically allocate resources, optimize routes, or develop targeted emergency response plans.

3.4. *Scenario-based resilience evaluation framework*

To evaluate the resilience of community-based service networks within the GCSN against diverse disruptions, this study formulates disruption scenarios covering three main aspects: individual disruptions, cumulative disruptions, and disruptions originating from hub ports affecting non-hub ones within the community. These scenarios are designed to mimic the impacts of real-world disruptive events such as natural disasters (e.g., hurricanes, tsunamis), cyberattacks, and geopolitical tensions (e.g., sanctions or blockades). Specifically, the individual disruption analysis aims to identify port characteristics that significantly impact the connectivity of community-based networks, often influenced by the localized intensity of natural disasters or targeted cyberattacks. The cumulative disruption assessment seeks to evaluate the collective effects of sequential disruptions, analogous to the escalating impacts of geopolitical tensions or a series of cyberattacks on multiple ports. Lastly, the reliance analysis focuses on assessing the residual connectivity of non-hub ports following the disruption of hub ones, reflecting how pivotal ports, if incapacitated by major events like blockades or large-scale natural disasters, affect the broader network within the relevant community.

3.4.1. *Individual disruption scenarios*

To evaluate the impact of individual port disruptions on community resilience, the reduction in $WDEC_A$ as per Eq. (13) is computed to determine the extent of connectivity degradation resulting from disconnecting each port from others in the GCSN. This analysis aids in determining the influence level on community resilience resulting from single-port attacks. Additionally, ports are categorized into groups based on factors like community relevance and hub functions to pinpoint the correlation between port attributes and their level of influence on community resilience.

3.4.2. *Cumulative disruption scenarios*

The essence of designing cumulative disruption scenarios lies in establishing the sequence for disrupting ports based on their importance. Typically, network topological metrics are utilized for analyzing port importance [14,48,49]. In this study, DC, CC, and BC are utilized and calculated as follows:

$$C_D(i) = \sum_{j=1}^{n} (a_{ij} + a_{ji}) \Big/ 2 \tag{14}$$

$$C_C(i) = \left(\frac{1}{\sum_{j=1}^{n} t_{ij,min}} + \frac{1}{\sum_{j=1}^{n} t_{ji,min}} \right) \Big/ 2 \tag{15}$$

$$C_B(i) = \sum_{i \neq j \neq q} \frac{g_{jq}(i)}{g_{jq}} \tag{16}$$

where $a_{ij} = 1$ if the is a direct connection from port i to j, otherwise $a_{ij} = 0$. $t_{ij,\mathrm{min}}$ represents the shortest transit time from port i to j, g_{jq} signifies the total number of paths with the shortest transit time from port j to q, and $g_{jq}(i)$ indicates the number of paths with the shortest transit time from port j to q, passing through port i. Similar to the resilience evaluation metrics, these network topological metrics also consider network directionality, while incorporating the weight (i.e., service capacity) of each link by employing the network disintegration model.

Additionally, the community membership attributes of each port are considered in the attack strategy design process, distinguishing between intra-community and inter-community ports. By integrating both the three topological metrics and the community membership attributes of the port, nine cumulative attack strategies are formulated: high DC attack scenario, hierarchical high DC attack scenario 1, hierarchical high DC attack scenario 2, high CC attack scenario, hierarchical high CC attack scenario 1, hierarchical high CC attack scenario 2, high BC attack scenario, hierarchical high BC attack scenario 1, and hierarchical high BC attack scenario 2. In the hierarchical attack scenario 1, intra-community ports are attacked first, followed by inter-community ports. Conversely, in the hierarchical attack scenario 2, inter-community ports are attacked first, followed by intra-community ports. For simplicity, these attack scenarios are denoted as DC1, DC2, DC3, CC1, CC2, CC3, BC1, BC2, and BC3 respectively in subsequent discussions.

The cumulative disruption scenarios systematically disrupt ports one by one according to pre-designed attack scenarios until all ports in the network are affected. To assess the collective impact of sequential port disruptions, a cumulative resilience measurement metric by extending Eq. (13) is devised as follows:

$$R\_WDEC = \frac{\sum_{i=1}^{N} WDEC_{post}^{i} \Big/ WDEC_{pre}}{N} \tag{17}$$

where $DWEC_{post}^{i}$ represents the residual community connectivity after attacking the first i ports in the disruption scenario, and N is the total number of ports within the GCSN. This metric measures the average residual community connectivity across different disruption levels. A slower reduction in the remaining network connectivity leads to a higher R_WDEC, indicating a greater resilience of the community to the corresponding cumulative attack scenario.

3.4.3. Dependence analysis of non-hub ports on hub ports

This subsection investigates the degree to which the connectivity of non-hub ports depends on the presence of hub ports within their community, shedding light on the importance of hub ports for connectivity enhancement. Here, the concept of the "survival connectivity ratio", utilized to quantify dependence [59], is employed. This ratio is calculated as the residual community connectivity of non-hub ports after attacking the hub ports within their community divided by the original community connectivity of non-hub ports without attacking the hub ports, which can be expressed as follows:

$$S\_WDEC_{A} = \frac{WDEC_{post}^{non-hub}}{WDEC_{pre}^{non-hub}} \tag{18}$$

where $WDEC_{pre}^{non-hub}$ and $WDEC_{post}^{non-hub}$ represent the connectivity among non-hub ports before and after attacking the hub ports. A low "survival connectivity ratio" indicates a high reliance on the connectivity provided by hub ports.

To examine the dependence of non-hub ports on hub ports under various disruptive circumstances, three simulation scenarios are devised. The first scenario entails severing all connections between the hub ports and other ports in the GCSN, simulating a complete shutdown of the hub ports following attacks. The second scenario gradually diminishes the level of connections between the hub ports and other ports by a fixed percentage, simulating the partial disruption of the hub ports and the consequent decrease in their cargo service capacity. The third scenario involves a sequential attack on hub ports in descending order, prioritized by their cargo service capacity, examining instances where multiple hub ports are disrupted cumulatively. By employing these structured scenarios and the defined "survival connectivity ratio", the reliance of non-hub ports on hub ports can be systematically explored.

4. Experimental results and discussion

4.1. Data collection and network construction

In this study, the global container shipping service data are collected from 'BIG SHIP DATA', a comprehensive database specializing in ocean sailing schedules, capacity, and service information, accessible at www.bluewaterreporting.com. Launched by ComPair Data, Inc., the database encompasses 2607 liner service routes from 298 ocean carriers. It provides one of the most comprehensive liner services databases available today, as found at www.compairdata.com, ensuring coverage of nearly all routes or regions [60]. A total of 13,266 shipping service records from the year 2022 are collected. Each data entry provides complete information on each service route, including details such as the original port, departure port, service frequency, deployed cargo service capacity (measured in TEUs), average sailing time from origin to departure, and the basic properties of ships sailing on this route. This comprehensive data simplifies the preprocessing steps required for analysis.

Utilizing this data, the weight of each shipping link is calculated by aggregating the corresponding transported port-to-port cargo service capacity, resulting in the creation of a weighted-directed GCSN. As illustrated in Fig. 3, the resulting GCSN visualization showcases 627 nodes, 3235 linked pairs, and 4174 directed links, covering most ports worldwide. Notably, the weighted-directed GCSN exhibits an asymmetric configuration, with 70.9 % of linked pairs unidirectionally connected and 97.8 % of linked pairs showing an unbalanced directed cargo service capacity. Furthermore, critical ports within the GCSN, such as Singapore and Shanghai in Asia, are identified based on their cargo service capacity, as outlined in Table 2. Particularly, Singapore Port demonstrates superior cargo service capacity compared to other ports. The establishment of a real-world shipping network and the identification of critical ports provide essential support for subsequent analyses of network resilience.

4.2. Port community structure analysis results

To achieve an effective community partition within the GCSN, it is imperative to first identify the hyperparameters within the SNMF model. Fig. 4 demonstrates the results of identifying two key input parameters: k and φ. In Fig. 4(a), the *Ncut* results with 20 randomly initialized H as inputs for each k are depicted. It is observed that the *Ncut* initially rises gradually at a slow pace and then shifts to a linear increase at a faster rate when it exceeds 10. This suggests that the elbow point occurs at $k = 10$, indicating that 10 is the optimal number of communities. Notably, the upper and lower boundaries depicted in the boxplot for each k exhibit a remarkable concentration, signifying the robust convergence and stability of the adopted optimization model, irrespective of the initial selection of H. Additionally, Fig. 4(b) illustrates the variation in the number of ports belonging to multiple communities and the number of ports belonging to at least one community as the membership threshold φ increases. It is evident that as φ increases, both indicators decrease, indicating a reduction in the overlap degree between communities. Specifically, when φ does not exceed 0.31, each port can be allocated to at least one community. The study aims to extract communities with distinct regionalization characteristics, thus necessitating the assurance of a low overlap degree between communities. Consequently, φ is ultimately set to 0.31 to guarantee each port is assigned to at least one community while maintaining a minimal overlap degree between communities.

Fig. 5 illustrates the geographical distributions of the identified community structures. As depicted, most communities comprise ports situated within the same area, with only a few communities including ports from different geographical areas but along the same international routes, as exemplified by Community 2. Overall, ports within the same community exhibit minimal spatial distances between them, while those from different communities demonstrate relatively larger distances. This observation suggests that the employed SNMF model effectively partitions the GCSN into several spatially compact communities. Additionally, the grey nodes represent ports belonging to more than one port community, strategically positioned between communities to facilitate connectivity. This underscores the effectiveness of the SNMF model in identifying overlapping port communities to some extent.

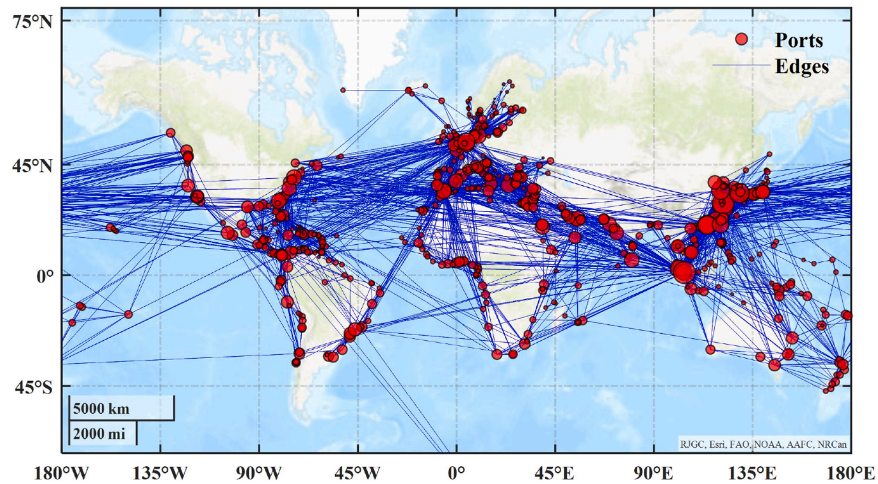

Fig. 3. Visualization of the weighted-directed GCSN, where the node size reflects each port's cargo service capacity.

Table 2
Top 20 ports ranked by cargo service capacity within the GCSN.

No.	Port name	Service capacity (Weekly TEU)	No.	Port name	Service capacity (Weekly TEU)
1	Singapore	1596,700	11	Kaohsiung	512,407
2	Shanghai	1507,213	12	Xiamen	464,933
3	Ningbo	1297,898	13	Antwerp	464,049
4	Busan	970,469	14	Tanjung Pelepas	416,940
5	Yantian	797,926	15	Nansha	379,371
6	Hong Kong	784,729	16	New York	371,411
7	Qingdao	721,892	17	Hamburg	371,222
8	Shekou	649,779	18	Dubai	356,018
9	Port Klang	614,003	19	Tanger	349,581
10	Rotterdam	597,303	20	Piraeus	316,768

Fig. 6 illustrates both the average cargo service capacity and average connection ratio for inter- and intra-community links of each generated port community, respectively. It is evident that the average cargo service capacity and the average connection ratio for inter-community links are significantly lower than for intra-community links, with the ratio of those for inter-community links to those for intra-community links not exceeding 8 %. This outcome exhibits dense intra-connection alongside sparse inter-connection, consequently indicating a superior community partitioning quality.

To further validate the effectiveness of the SNMF model employed for community detection, Fig. 7 presents a comparison between SNMF and other current methods. Among these, Spectral [30] and SNMF allow for the manual control of cluster numbers, whereas other methods automatically determine the number of clusters. Experimental results show that the final number of clusters for Clique Percolation [14] is 10 (when the clique size is 3), for Louvain [17,33] it ranges between 9–11 with the majority around 10 (above 70 %), and for Infomap [16,31], it varies between 49–51. Considering the need for consistency in comparative analysis and the research objective to analyze larger, more structurally distinct communities rather than fragmented smaller clusters, the experiments focus on comparisons where the cluster count is set to 10, aligning with the optimal cluster number determined by SNMF. Each method is run repeatedly 20 times. As depicted in Fig. 7, SNMF significantly outperforms the other three methods in terms of *Ncut* values, which reaffirms the superiority of the employed method.

Additionally, Fig. 8 displays the visualized memberships of each port belonging to different communities using normalized *H*. This visualization effectively showcases the capability of normalized *H* to discern the community membership distribution of each port, thereby facilitating explicit assignment of each port to multiple communities. Such a finding suggests that *H* extracted via SNMF serves as a promising solution, demonstrating its inherent superiority in soft clustering and robust capacity to uncover overlapping community structures. This stands in contrast to alternative methods such as the Infomap algorithm [16] and Louvain algorithm [17].

Table 3 presents the basic statistical characteristics of each detected

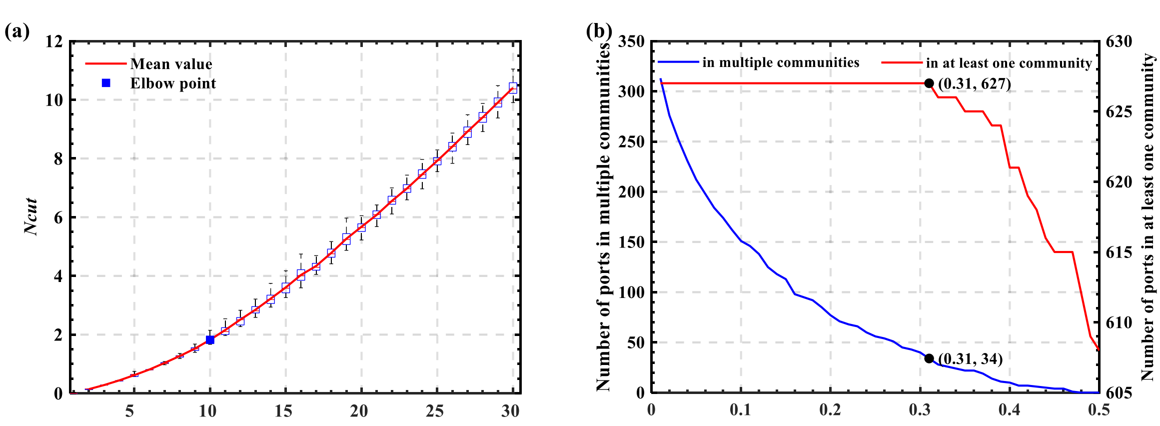

Fig. 4. Hyperparameter identification in community detection model. (a) Influence of the number of communities on *Ncut*; (b) influence of the membership threshold on the number of ports belonging to multiple communities and the number of ports belonging to at least one community.

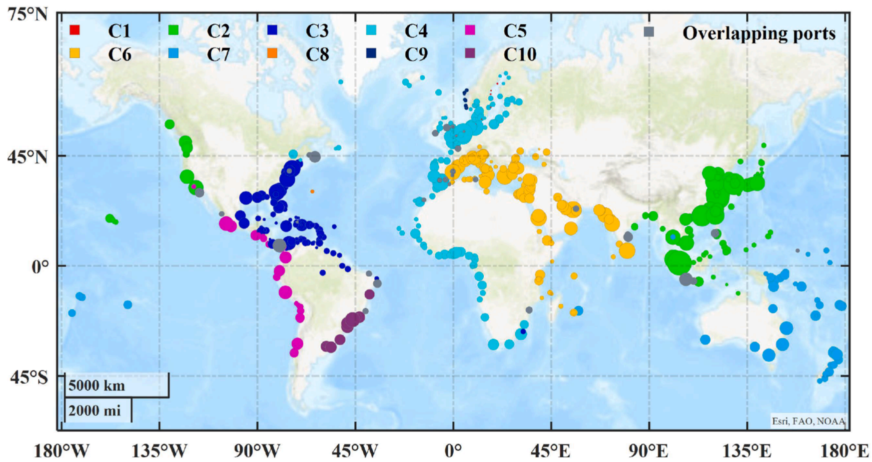

Fig. 5. Visualization of port community detection results.

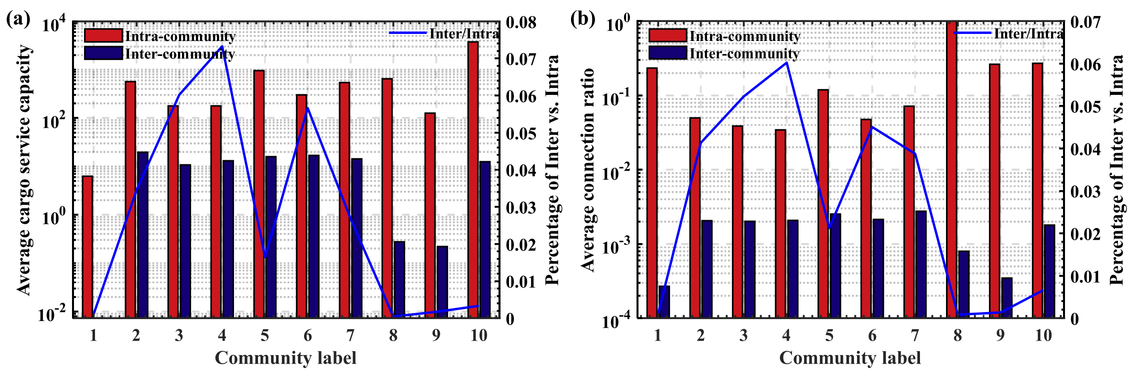

Fig. 6. (a) Average cargo service capacity for intra- and inter-community links; (b) average connection ratio for intra- and inter-community links.

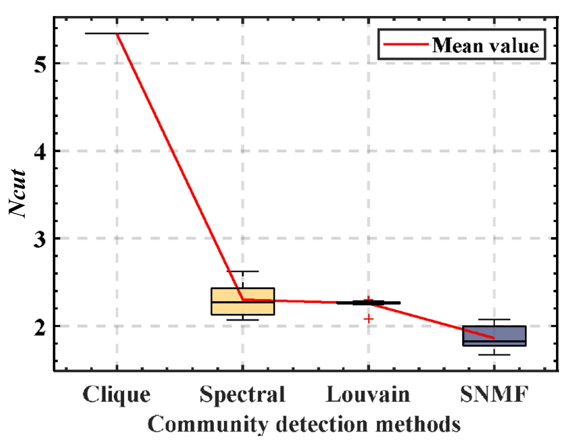

Fig. 7. Comparisons of SNMF with other currently used methods for port community detection.

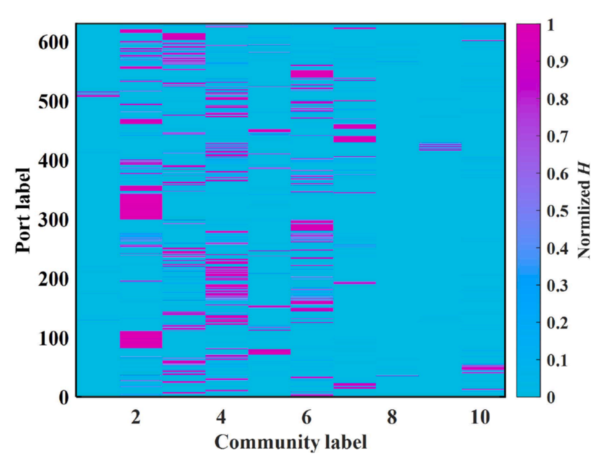

Fig. 8. Visualization of memberships of each port within different communities in terms of normalized *H*.

community. It reveals that both intra-community cargo service capacity and intra-community connections significantly surpass those between communities, aligning with the insights depicted in Fig. 6. Even with the removal of inter-community links, each community maintains a substantial share of cargo service capacity (59 %–83 %) and connections (57 %–80 %). This observation underscores one of the characteristics of the GCSN structure, revealing its regionalization nature, and emphasizes the necessity to prioritize intra-cluster connectivity and conduct resilience analysis from a regional community perspective. Additionally, the distribution of ports within each community exhibits variation, including four large-scale, two moderate-scale, and four small-scale communities, highlighting the spatial heterogeneity inherent in port communities. This also implies the efficacy of the SNMF model in simultaneously detecting both large and small communities without resolution constraints, thereby facilitating the extraction of fine-grained hierarchical port community structures from the GCSN. Given the limited connectivity in smaller communities, subsequent resilience analyses are directed towards the six large-scale and moderate-scale communities: East Asia-North America West (C2), North America East (C3), Northwest European-West Africa (C4), South America East (C5),

Table 3
Statistical characteristics of each port community.

No.	Number of ports	Cargo service capacity (Weekly TEU)			Number of connections			Community size
		Total	Intra-	Inter-	Total	Intra-	Inter-	
1	6	243	189 (78 %*)	54 (22 %)	9	7 (78 %)	2 (22 %)	Small
2	157	16,805,909	13,913,523 (83 %)	2892,385 (17 %)	1525	1221 (80 %)	304 (20 %)	Large
3	121	3912,812	2595,423 (66 %)	1317,390 (34 %)	811	563 (69 %)	248 (31 %)	Large
4	146	5588,492	3760,679 (67 %)	1827,813 (33 %)	1019	728 (71 %)	291 (29 %)	Large
5	35	1787,955	1134,336 (63 %)	653,619 (37 %)	247	142 (57 %)	105 (43 %)	Medium
6	126	6850,429	4713,177 (69 %)	2137,251 (31 %)	1018	748 (73 %)	270 (27 %)	Large
7	46	1879,872	1111,869 (59 %)	768,002 (41 %)	296	148 (50 %)	148 (50 %)	Medium
8	2	1993	1303 (65 %)	690 (35 %)	4	2 (50 %)	2 (50 %)	Small
9	7	7177	5263 (73 %)	1914 (27 %)	14	11 (79 %)	3 (21 %)	Small
10	15	1016,429	788,324 (78 %)	228,104 (22 %)	90	57 (63 %)	33 (37 %)	Small

* The value in a bracket indicates the ratio between Intra- or Inter-port community and the total.

Mediterranean-Middle East (C6), and Oceania (C7).

Based on the hub port identification indicators (Eqs. (4)-(6)), three types of hub ports within the GCSN are further distinguished. Their geographical distribution is visualized in Fig. 9. It is observed that most provincial hubs possess extensive immediate hinterlands within their corresponding port communities. Gateway hubs, on the other hand, tend to cluster near canals and straits, with the majority also serving as provincial hubs. These dual-function ports act as crucial nodes for both intra- and inter-regional shipping, enabling smooth cargo transshipment within and between communities. Regarding Connector hubs, ports including Singapore and New York stand out, each with P_i exceeding 0.69. Notably, they possess three hub identities simultaneously and are ranked among the top 20 ports in terms of cargo service capacity (refer to Table 2). The two pivotal ports nurture robust interregional shipping networks, fostering equitable connections among diverse port communities and facilitating container transshipment. The numerical distribution of provincial, gateway, and connector hubs across the six examined communities is showcased in Fig. 10.

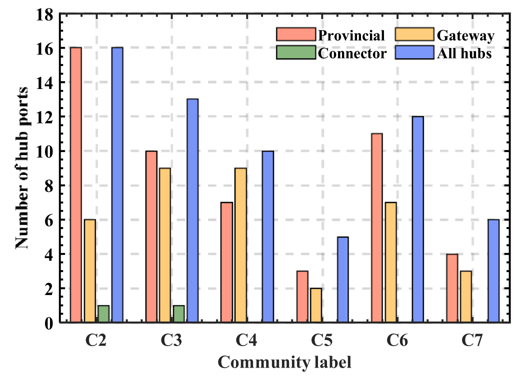

Fig. 10. Number of hub ports in each community.

4.3. Scenario-based resilience assessment results

4.3.1. Simulation results of individual disruptions

Table 4 presents the impact of individual disruptions on community resilience, considering the community membership characteristics of the attacked ports. As shown in the table, deliberate attacks on individual intra-community ports have a substantial effect on the corresponding community across all six resilience metrics in Eq. (13). Specifically, these attacks can result in a maximum $WDE_{A,intra}$ loss of 11.35–27.12 %, a maximum $WDE_{A,inter}$ loss of 6.36–13.59 %, a maximum $WDE_{A,all}$ loss of 8.32–15.78 %, a maximum $WDC_{A,intra}$ loss of 9.36–24.89 %, a maximum $WDC_{A,inter}$ loss of 4.74–12.14 %, and a maximum $WDC_{A,all}$ loss of 5.83–13.09 % for each community, respectively. In contrast, deliberate attacks on individual inter-community ports primarily affect inter-community resilience metrics rather than intra-community ones. Additionally, the average impact of individual intra-community attacks is significantly greater than that of individual inter-community attacks across $WDEC_A$. Importantly, deliberate individual intra-community attacks on C5 should be prioritized due to the most significant degradation across $WDEC_A$. These findings underscore the sensitivity of port communities to deliberate individual disruptions, particularly intra-community port attacks, highlighting the need for targeted measures to prevent deliberate individual disruptions, thereby preserving community network connectivity and preventing economic losses.

Table 5 illustrates the average impact of individual disruptions on community resilience, considering the hub roles of the attacked ports.

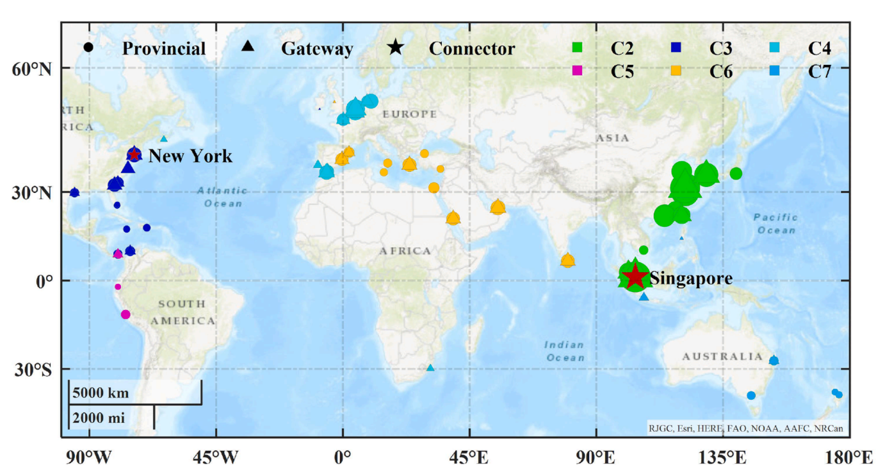

Fig. 9. Geographical distribution of hub ports within the GCSN.

Table 4
Reduction in $WDEC_A$ under individual port disruptions: Perspectives on intra-community port and inter-community port attacks.

Type of ports	Reduction in $WDE_{A,intra}$ (%)					
	C2	C3	C4	C5	C6	C7
Intra (max)	13.81	12.83	18.49	27.12	11.35	19.6
Inter (max)	0.29	0.88	0.42	0.97	0.60	2.89
Intra (average)	1.67	2.28	1.80	7.51	2.14	6.22
Inter (average)	0.00	0.01	0.01	0.00	0.01	0.01

Type of ports	Reduction in $WDC_{A,intra}$ (%)					
	C2	C3	C4	C5	C6	C7
Intra (max)	12.96	9.54	10.54	24.89	9.36	13.86
Inter (max)	0.60	1.58	1.57	1.46	2.22	4.01
Intra (average)	1.69	2.24	1.83	7.69	2.13	5.87
Inter (average)	0.01	0.02	0.01	0.01	0.02	0.03

Type of ports	Reduction in $WDE_{A,inter}$ (%)					
	C2	C3	C4	C5	C6	C7
Intra (max)	11.29	7.74	7.04	13.59	6.36	10.38
Inter (max)	5.51	4.24	5.30	7.07	7.07	15.65
Intra (average)	1.00	1.28	1.03	4.34	1.17	3.21
Inter (average)	0.34	0.34	0.34	0.30	0.32	0.30

Type of ports	Reduction in $WDC_{A,inter}$ (%)					
	C2	C3	C4	C5	C6	C7
Intra (max)	7.75	5.95	5.49	12.14	4.74	7.52
Inter (max)	2.78	3.09	5.05	4.01	5.87	5.43
Intra (average)	0.87	1.16	0.95	4.03	1.07	3.00
Inter (average)	0.31	0.29	0.30	0.25	0.30	0.26

Type of ports	Reduction in $WDE_{A,all}$ (%)					
	C2	C3	C4	C5	C6	C7
Intra (max)	12.5	9.15	11.65	15.78	8.32	10.93
Inter (max)	2.15	2.87	3.20	5.71	4.00	12.46
Intra (average)	1.43	1.65	1.34	5.05	1.63	3.96
Inter (average)	0.12	0.22	0.21	0.23	0.17	0.23

Type of ports	Reduction in $WDC_{A,all}$ (%)					
	C2	C3	C4	C5	C6	C7
Intra (max)	9.37	6.14	6.47	13.09	5.83	8.14
Inter (max)	1.92	2.62	4.38	3.77	5.00	5.25
Intra (average)	1.12	1.33	1.12	4.30	1.32	3.28
Inter (average)	0.22	0.24	0.24	0.23	0.23	0.23

The table reveals a significant discrepancy in the impact on community network resilience between attacks on hub ports and non-hub ports. Attacking a single hub port results in a substantial decline in the original community connectivity. Conversely, attacking individual non-hub ports has a somewhat lesser impact on the original community connectivity. For instance, compared to attacking non-hub ports, the average reduction in $WDE_{A,intra}$ of C2 when attacking single provincial hubs, gateway hubs, and connector hubs is approximately 37, 43, and 30 times greater, respectively. Additionally, the extent of impact varies when attacking different types of hub ports, with provincial hubs and gateway hubs exerting a more significant impact compared to connector hubs. This variance may be attributed to the fact that provincial hubs and gateway hubs are contained within their respective communities, while connector hubs are identified from a global network perspective and may not necessarily be part of the specific community. The substantial impact of connector hubs on the community typically becomes apparent when they are included in the corresponding community. Nevertheless, their impact remains significantly greater than that of non-hub ports. This analysis highlights the importance of identifying hub ports in terms of the community structures of the GCSN, while emphasizing the critical need to maintain the undisturbed status of hub ports to ensure the shipping connectivity of port communities. More detailed exploration on the impact of individual disruptions can be found in Appendix A.

4.3.2. Simulation results of cumulative disruptions

Fig. 11 illustrates the R_WDEC of various communities under nine cumulative attack scenarios, showcasing their respective impact. To comprehensively evaluate the degree of influence of these scenarios, Fig. 12 further depicts the average R_WDEC across all investigated communities. Analysis of the figure reveals several key phenomena. Firstly, scenarios DC2, CC2, and BC2 (i.e., hierarchical scenarios 1) exhibit the most significant impact on R_WDEC, followed by DC1, CC1, and BC1, whereas DC3, CC3, and BC3 (i.e., hierarchical scenarios 2) exert the weakest influence. Particularly noteworthy is the significant reduction in R_WDEC values to less than 0.03 for scenarios DC2, CC2, and BC2, and below 0.13 for scenarios DC1, CC1, and BC1, warranting increased attention. Moreover, the disruption impact of the three metrics (i.e., DC, CC, and BC) are observed to be relatively similar, with a general ranking of DC, BC, and CC, as depicted by the mean rank in Fig. 12. Secondly,

Table 5
Reduction in $WDEC_A$ under individual port disruptions: Perspectives on hub port and non-hub port attacks.

Role of ports	Average $WDE_{A,intra}$ reduction (%)					
	C2	C3	C4	C5	C6	C7
Provincial hubs	8.15	8.99	12.29	18.59	7.19	15.16
Gateway hubs	9.47	9.04	8.65	11.97	6.94	6.99
Connector hubs	6.6	6.04	0.25	0.00	0.27	1.45
Not hub ports	0.22	0.28	0.28	0.3	0.31	0.36
All ports	0.42	0.45	0.42	0.42	0.44	0.47

Role of ports	Average $WDC_{A,intra}$ reduction (%)					
	C2	C3	C4	C5	C6	C7
Provincial hubs	6.57	6.61	6.99	16.07	6.1	10.08
Gateway hubs	8.05	6.58	5.84	12.42	6.12	6.57
Connector hubs	6.59	3.64	1.13	0	1.11	1.78
Not hub ports	0.27	0.33	0.35	0.32	0.34	0.38
All ports	0.43	0.45	0.44	0.44	0.44	0.46

Role of ports	Average $WDE_{A,inter}$ reduction (%)					
	C2	C3	C4	C5	C6	C7
Provincial hubs	3.41	4.91	5.28	9.47	4.02	5.82
Gateway hubs	4.61	4.51	4.51	12.30	4.32	6.61
Connector hubs	6.55	3.99	3.32	2.07	4.26	8.14
Not hub ports	0.43	0.44	0.43	0.44	0.42	0.43
All ports	0.51	0.52	0.5	0.52	0.49	0.51

Role of ports	Average $WDC_{A,inter}$ reduction (%)					
	C2	C3	C4	C5	C6	C7
Provincial hubs	2.79	3.85	4.28	8.16	3.04	5.17
Gateway hubs	3.82	3.86	3.63	8.21	3.09	3.84
Connector hubs	4.63	4.52	3.24	1.74	3.53	3.05
Not hub ports	0.39	0.39	0.39	0.39	0.4	0.41
All ports	0.45	0.46	0.45	0.46	0.45	0.46

Role of ports	Average $WDE_{A,all}$ reduction (%)					
	C2	C3	C4	C5	C6	C7
Provincial hubs	6.46	6.44	8.1	11.5	5.51	8.16
Gateway hubs	7.73	6.21	6.18	12.23	5.55	6.7
Connector hubs	6.58	4.76	2.08	1.61	2.39	6.47
Not hub ports	0.29	0.38	0.37	0.41	0.37	0.41
All ports	0.45	0.49	0.47	0.5	0.47	0.5

Role of ports	Average $WDC_{A,all}$ reduction (%)					
	C2	C3	C4	C5	C6	C7
Provincial hubs	3.96	4.29	4.8	8.76	3.76	5.66
Gateway hubs	5.13	4.29	4.06	8.52	3.81	4.11
Connector hubs	5.24	4.38	2.83	1.61	2.96	2.93
Not hub ports	0.35	0.38	0.38	0.39	0.38	0.41
All ports	0.44	0.45	0.45	0.46	0.45	0.46

scenarios DC1, CC1, BC1, DC3, CC3, and BC3 demonstrate the most significant impact on inter-community resilience metrics, followed by overall-community resilience metrics, with the least impact on intra-community resilience metrics. Conversely, scenarios DC2, CC2, and BC2 affect intra-community metrics the most, followed by overall-community metrics, with minimal impact on inter-community metrics. Thirdly, it is noted that intra-community resilience metrics exhibit the greatest fluctuations across different attack scenarios, followed by overall-community resilience metrics, while inter-community resilience metrics display the least fluctuations, indicating the highest sensitivity of intra-community resilience metrics to attack scenario selection. Further insights into the impact of various cumulative attack scenarios on community resilience can be found in Appendix B.

4.3.3. Dependence results of non-hub ports on hub ports

Fig. 13 illustrates the survival connectivity ratios of non-hub ports following the complete disruptions of all hub ports within the relevant community. As depicted, hub ports play a crucial role in the connectivity of non-hub ports, evidenced by a significant decline in connectivity among non-hub ports across all communities when all hub ports cease operation, despite each community's hub ports comprising no more than 15 %. Particularly noteworthy is the notably low S_WDEC_A of non-hub ports in C2, ranging from 40 % to 60 %, indicating their heavy reliance on hub ports for connectivity. Additionally, it is observed that connection efficiency metrics are more significantly affected than connection extent metrics, owing to their distinct measurement functions. Connection efficiency metrics prioritize the shortest service connection time. Closure of hub ports leads to a significant increase in the shortest transit time between two non-hub ports. Conversely, connection extent metrics focus on accessibility between ports, wherein two non-hub ports may remain accessible via alternate paths due to the substitution effect among indirect connection links when hub ports are closed. Overall, the community network functions akin to a "hub-and-spoke system", with hub ports serving as bridges that govern connectivity among non-hub ports.

In practice, ports often experience partial disruptions rather than complete shutdowns. Consequently, it is essential to evaluate the impact of partial disruptions to hub ports on the connectivity among non-hub ports. Fig. 14 illustrates the variation in S_WDEC_A of non-hub ports as hub ports within the relevant community undergo partial disruptions by reducing their cargo service capacity. The figure reveals an approximately linear relationship between the disruption level of hub ports and

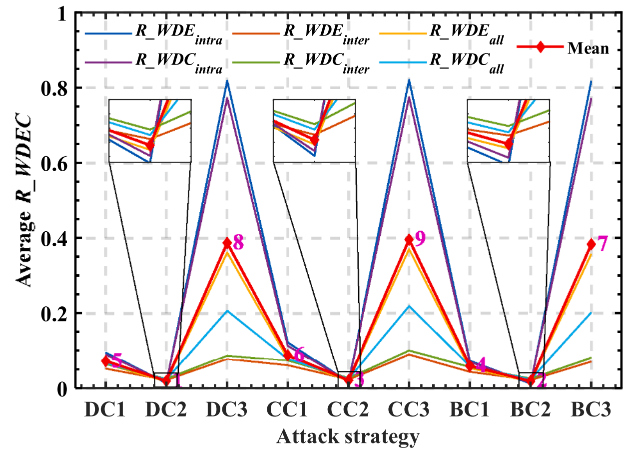

Fig. 12. Average R_WDEC of all investigated communities under different cumulative attack scenarios.

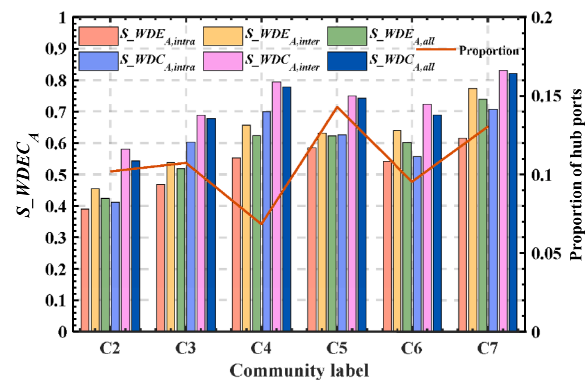

Fig. 13. S_WDEC_A of non-hub ports following the complete disruption of all hub ports within the relevant community.

S_WDEC_A, with slight deviations observed at certain points. This analysis provides insights into the evolution of connectivity among non-hub ports amidst varying degrees of hub port disruptions.

Furthermore, Fig. 15 illustrates the cumulative effects of hub port disruptions on non-hub ports. The hub ports are continuously targeted in

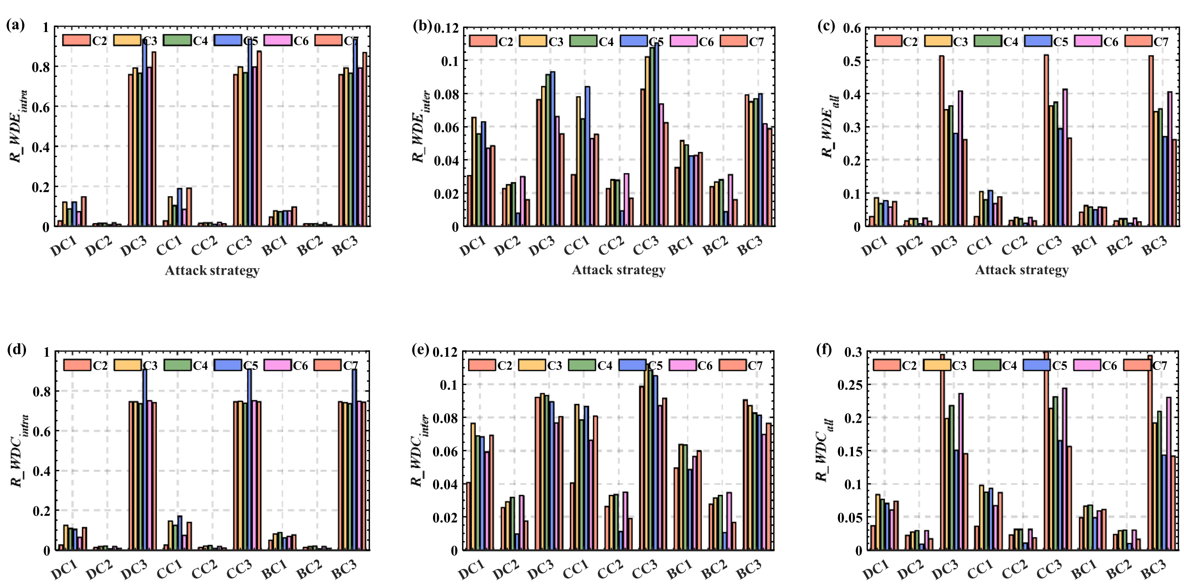

Fig. 11. R_WDEC of different communities under different cumulative attack scenarios.

descending order based on their cargo service capacity. It is apparent that the variation in S_WDEC_A for different communities varies significantly, indicating distinct coupling effects when different multiple hub ports are disrupted. Additionally, the observations once again underscore the significant influence of multiple hub port disruptions. For instance, the shutdown of the first four hub ports in C2 and the first two hub ports in C5 can severely impact the original connectivity of non-hub ports. Moreover, a ladder shape is discernible in C5, suggesting that additional cumulative disruptions to certain hub ports do not necessarily further diminish connectivity among non-hub ports, possibly due to alternative connections among them. However, it is crucial to note that the simultaneous complete disruptions of all hub ports can significantly degrade the connection performance of non-hub ports, warranting careful consideration.

4.4. Discussions and practical implications

Building on the above analyses, this section synthesizes the key findings and highlights their real-world significance for port operators, shipping companies, and policymakers, respectively. The proposed resilience assessment framework reveals how port community structures, hub-spoke relationships, and disruption scenarios jointly shape the robustness of shipping network. These insights move beyond purely theoretical metrics by demonstrating how stakeholders can leverage the findings to enhance decision-making and risk-management strategies in complex maritime contexts.

(1) Identifying critical ports and strengthening targeted protections

A major takeaway is the disproportionate influence of hub ports, particularly those with high intra-community connectivity, on network stability. Results from individual and cumulative disruption scenarios show that targeted attacks or failures of these hub ports (e.g., gateway hubs and provincial hubs) can trigger significant connectivity losses in their respective communities. In practice, port authorities and shipping companies can use these insights to prioritize resilience investments, such as infrastructure upgrades, enhanced security measures, or backup operational capacity, where they are most needed. For instance, establishing redundant routes, stockpiling essential equipment, or deploying rapid-response teams at top-ranked hub ports can help minimize downtime and economic losses in the event of critical node failures.

(2) Supporting strategic resource allocation and contingency planning

The community-based resilience assessment approach clarifies how local disruptions can have broader regional ramifications, depending on the interplay between intra- and inter-community connections. By quantifying the impact of different disruption scales (individual port failures, partial capacity losses, or simultaneous multi-port shutdowns), the framework aids stakeholders in balancing limited resources against diverse risk scenarios. Shipping companies and policymakers, for example, can develop tiered emergency protocols that scale in intensity depending on the severity of port disruptions. This ensures that response measures, ranging from rerouting vessels to temporarily shifting cargo operations, are both cost-effective and proportionate to the actual threat.

(3) Enhancing policy development and long-term network planning

In addition to informing short-term response tactics, the metrics and simulations presented also guide broader policy and planning decisions. Policymakers can integrate the findings into maritime infrastructure development programs, ensuring that investments in new or expanded ports strengthen regional connectivity without over-reliance on a single hub. Likewise, shipping alliances and port authorities might use these results when negotiating route structures or planning for emerging corridors (e.g., Arctic passages) to safeguard the overall resilience of the GCSN. Periodic re-assessments using updated service data would allow decision-makers to track how evolving trade patterns or geopolitical shifts influence network vulnerabilities over time.

(4) Facilitating cross-sector collaboration and future research

Finally, the community-focused perspective underscores a need for collaborative resilience efforts across ports and shipping lines. Because disruptions at hub ports can ripple through entire communities, enhanced information sharing, coordinated contingency exercises, and joint investments in port readiness are vital. Future studies could refine these

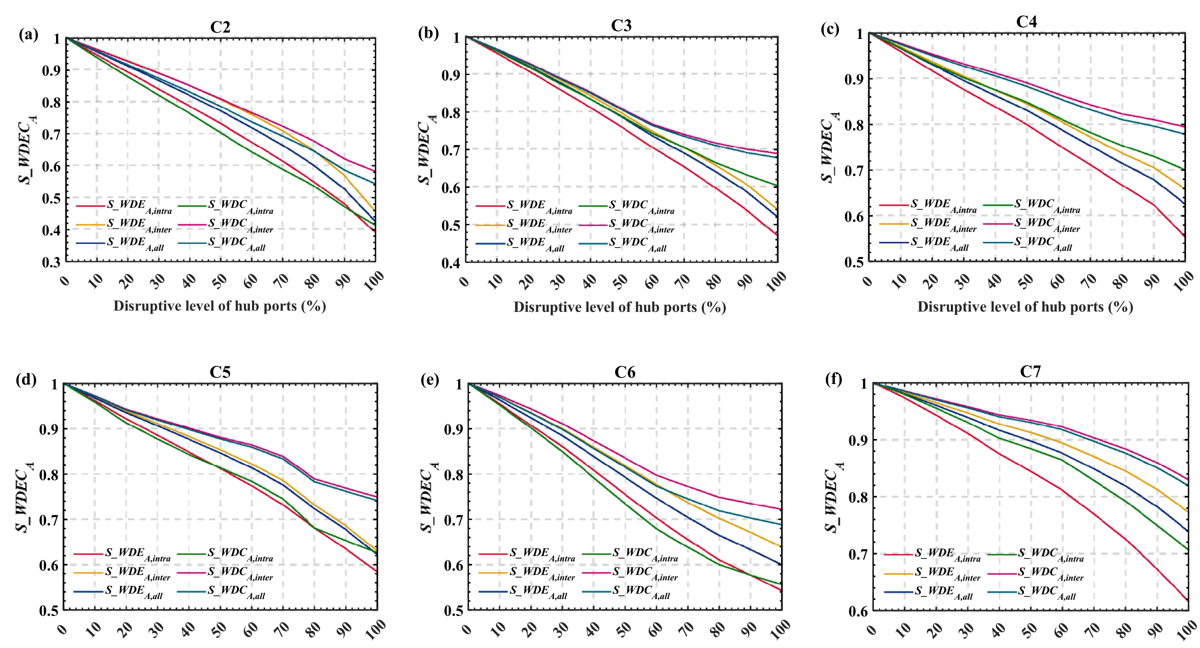

Fig. 14. Variation in S_WDEC_A of non-hub ports when the hub ports within the relevant community are attacked at different levels. (a) C2; (b) C3; (c) C4; (d) C5; (e) C6; (f) C7.

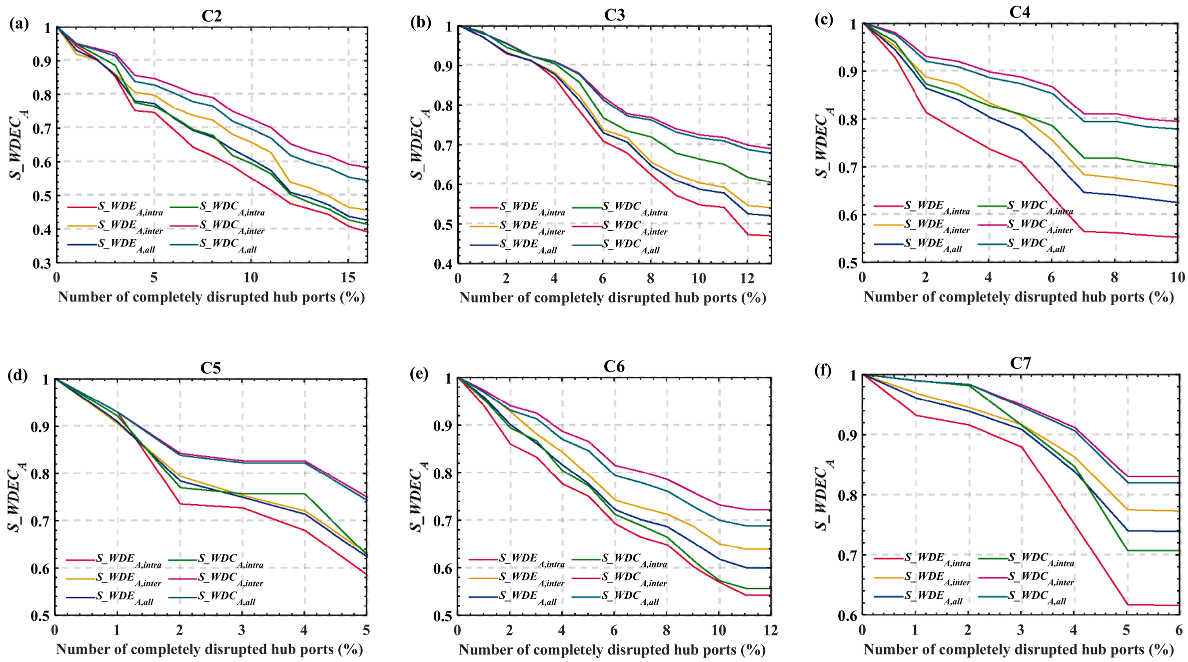

Fig. 15. Variation in S_WDEC_A of non-hub ports when hub ports are continuously attacked in descending order in terms of their cargo service capacity. (a) C2; (b) C3; (c) C4; (d) C5; (e) C6; (f) C7.

methods by examining multi-commodity flows, real-time disruption data, or climate-related risks such as extreme weather events and rising sea levels. By continually integrating these factors, practitioners can obtain an evolving, data-driven blueprint for managing uncertainty and safeguarding the stability of maritime trade networks worldwide.

Overall, this refined understanding of network structure and hub-port vulnerabilities offers actionable guidance for real-world resilience strategies. By uncovering community structures, pinpointing critical nodes, and quantifying disruption impacts, the proposed framework equips industry and government stakeholders with the tools necessary to build more robust shipping networks in an era of heightened global uncertainty.

5. Conclusion

Resilience assessment for the GCSN is a critical element for enhancing readiness to address potential disruption risks. This study presents a holistic methodology for resilience assessment of the GCSN from a community-based perspective, featuring the following distinctive elements: 1) Introduction of an advanced graph-based clustering algorithm to uncover fine-grained overlapping community structures within the GCSN, thereby enhancing understanding of its architecture; 2) Development of six novel community-based resilience metrics that incorporate network directionality and link weight, enabling effective measurement of the community networks' ability to maintain both connection efficiency and extent across intra-community, inter-community, and overall community aspects; and 3) Design of various disruption simulation scenarios, encompassing individual disruptions, cumulative disruptions, and disruptions originating from hub ports affecting non-hub ports, to systematically evaluate community resilience while incorporating the disrupted port characteristics such as community membership distribution, functional attributes, and topological properties.

Experimental analyses based on global container shipping service data validate the effectiveness of the methodology and reveal several key findings: 1) 10 communities of varying sizes are identified, each maintaining a significant share of cargo service capacity (59 %−83 %) and connections (57 %−80 %) through intra-community links alone, highlighting a strong regionalization effect; 2) Attacks on single intra-community hub ports can have a disproportionately large impact compared to attacks on inter-community non-hub ports, with resilience degradation even being several tens of times greater in the former; 3) Under specific hierarchical scenarios (e.g., DC2, CC2, BC2), the cumulative resilience measurement metric (*R_WDEC*) for communities can drop below 3 %, and even simultaneous disruptions at a few key ports can lead to the collapse of community network connectivity; 4) A complete shutdown of all hub ports within a community can reduce the connectivity of non-hub ports by 40–60 % in certain regions, suggesting that the community network functions akin to a 'hub-and-spoke' system, with hub ports serving as critical connectivity bridges for non-hub ports. Subsequent discussions and implications analyses provide significant insights for stakeholders and decision-makers, aiding in understanding the dynamics of shipping network resilience, informing strategic decisions to mitigate disruption risks, and evaluating the effectiveness of proposed strategies and policies.

Potential future research can explore several key areas. Firstly, further investigation is needed into how the characteristics of port community network structures, such as network configuration, spatial heterogeneity, and function allocation, impact network resilience. This exploration can assist stakeholders in devising tailored disruption mitigation strategies to adapt to the unique features of different community networks. Second, analyzing the cascading effects of port failures under different cargo flow redistribution rules is vital to understanding the complex interdependencies among ports in community networks, especially when numerous transportation routes are simultaneously rerouted due to multiple port disruptions. Thirdly, it is imperative to delve deeply into the development of models aimed at enhancing resilience recovery. These models should comprehensively consider factors such as network structure, resource deployment, demand, and cost. By incorporating such considerations, researchers can devise more practical, effective, and fault-tolerant recovery and enhancement strategies for port network resilience.

CRediT authorship contribution statement

Xuri Xin: Writing – review & editing, Writing – original draft, Visualization, Validation, Software, Methodology, Investigation, Formal analysis, Data curation, Conceptualization. **Zaili Yang:** Writing – review

& editing, Supervision, Resources, Project administration, Funding acquisition, Formal analysis, Data curation, Conceptualization.

Declaration of competing interest

The authors declare that they have no known competing financial interests or personal relationships that could have appeared to influence the work reported in this paper.

Acknowledgments

This research was funded by a European Research Council project under the European Union's Horizon 2020 research and innovation program (Grant Agreement No. 864724).

Appendix A. Detailed analysis of the impact of individual port disruptions on community resilience

To explore the impact of individual disruptions in more detail, Fig. A1 illustrates the resilience impact of each port's disruption on the East Asia-North America West Community (C2). These figures display the DC, CC, and BC metrics of each port alongside their functional attributes and community membership characteristics. Several noteworthy observations emerge. Firstly, the proportion of ports significantly impacting the resilience of C2 under individual disruptions is remarkably small, predominantly comprising intra-community hub ports with high DC, CC, and BC, highlighting the heterogeneous distribution of their influences. Secondly, notable correlations exist between a port's topological characteristics (i.e., DC, CC, BC) and its disruptive impact. However, the correlation strength varies significantly for intra-community and inter-community ports, with intra-community ports exerting a stronger positive correlation compared to inter-community ports, consistent with observations from Table 4. Particularly, individual port attacks from outside the community exhibit negligible effects on intra-community resilience metrics (i.e., $WDE_{A,intra}$ and $WDC_{A,intra}$), as evidenced by the clustering of light red markers near zero along the vertical axis in Fig. A1(a) and (b). Thirdly, the Singapore port holds a pivotal position within C2, wielding utmost influence across all six resilience metrics owing to its multifaceted hub functions. In summary, the community network displays low resilience against potential individual disruptions from intra-community hub ports, underscoring the importance of safeguarding their operational integrity to mitigate potential influence within the community network.

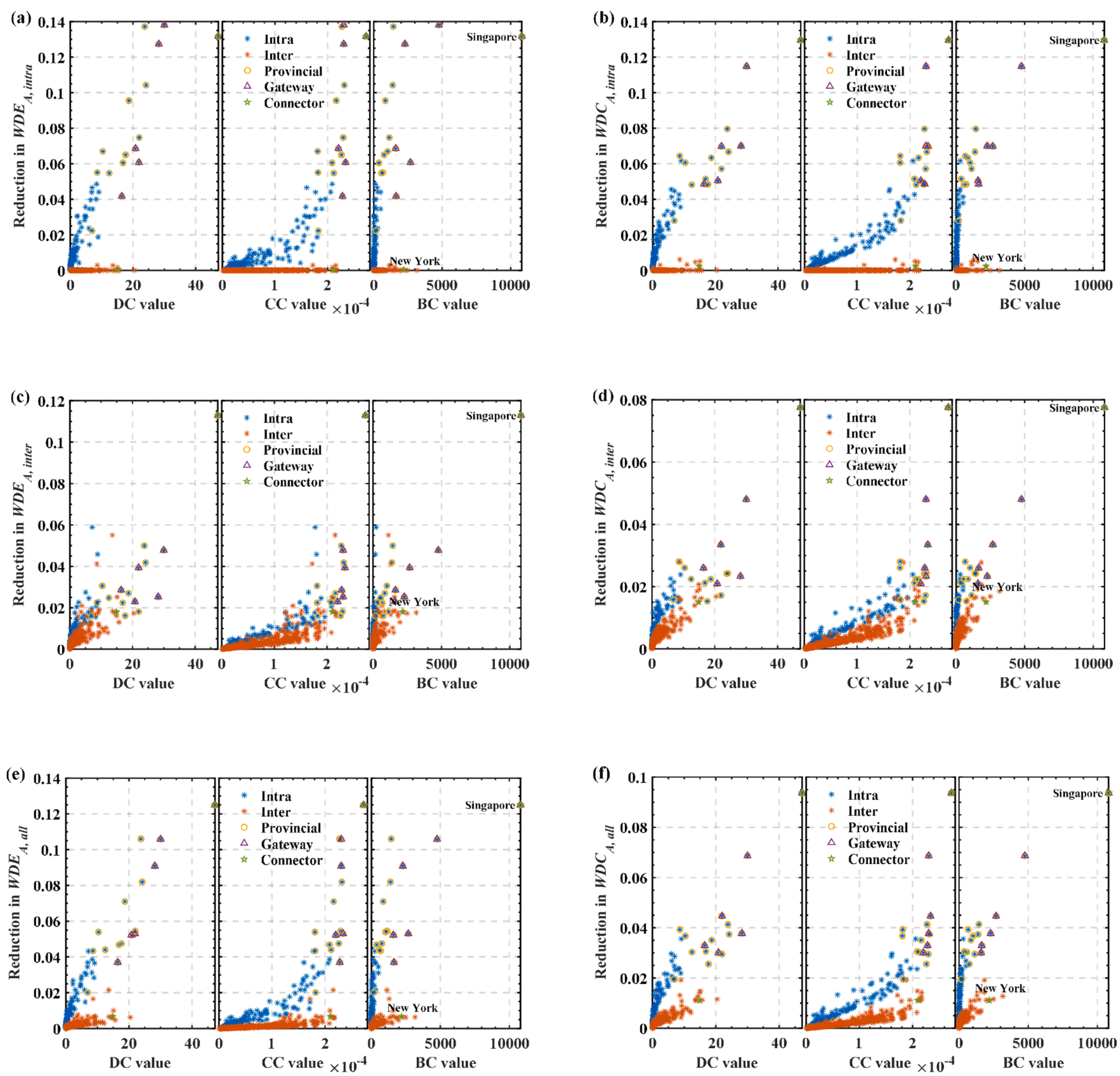

Fig. A1. Reduction in $WDEC_A$ of C2 with individual port disruptions.

Appendix B. Detailed analysis of the impact of cumulative port disruptions on community resilience

To gain deeper insights into the impact of various cumulative attack scenarios on community resilience, Fig. B1 presents an illustrative example focusing on the East Asia-North America West (C2), showcasing the fluctuation of $WDEC_A$ under continuous port attacks across the proposed nine scenarios. The figures demonstrate a sharp reduction in $WDEC_A$ when implementing continuous port disruptions based on the attack order in scenarios DC2, CC2, BC2, DC1, CC1, and BC1, with curves declining rapidly and then flattening out. Notably, under scenarios DC2, CC2, and BC2 (i.e., hierarchical scenarios 1), even the simultaneous disruptions of a few key ports can result in the collapse of community network connectivity. For instance, the $WDE_{A,intra}$ metric of C2 shapely diminishes to approximately 73 %, 62 %, and 54 % when the first two, three, and four ports are disrupted under scenario DC2, as depicted in the subfigure of Fig. B1(a). It is evident that the ports prioritized for attack are hub ports, emphasizing the vulnerability of the community network to deliberate and continuous disruptions targeting hub ports. Unfortunately, the concentration of hub ports in a single region, such as East Asia (as indicated in Fig. 9), renders the network susceptible to simultaneous disruptions through human-led attacks or regional natural disasters. Conversely, in cumulative scenarios DC3, CC3, and BC3, a slower reduction in $WDEC_A$ occurs even with a significant number of ports disrupted. This suggests a higher resilience of community network connectivity under hierarchical scenarios 2, attributable to the weaker impact of inter-community ports on community network connectivity, allowing the network to remain well interconnected despite continuous disruptions. Consequently, strategies must prioritize preventing the simultaneous failures of intra-community hub ports, while disruptions to inter-community ports can be of lesser concern.

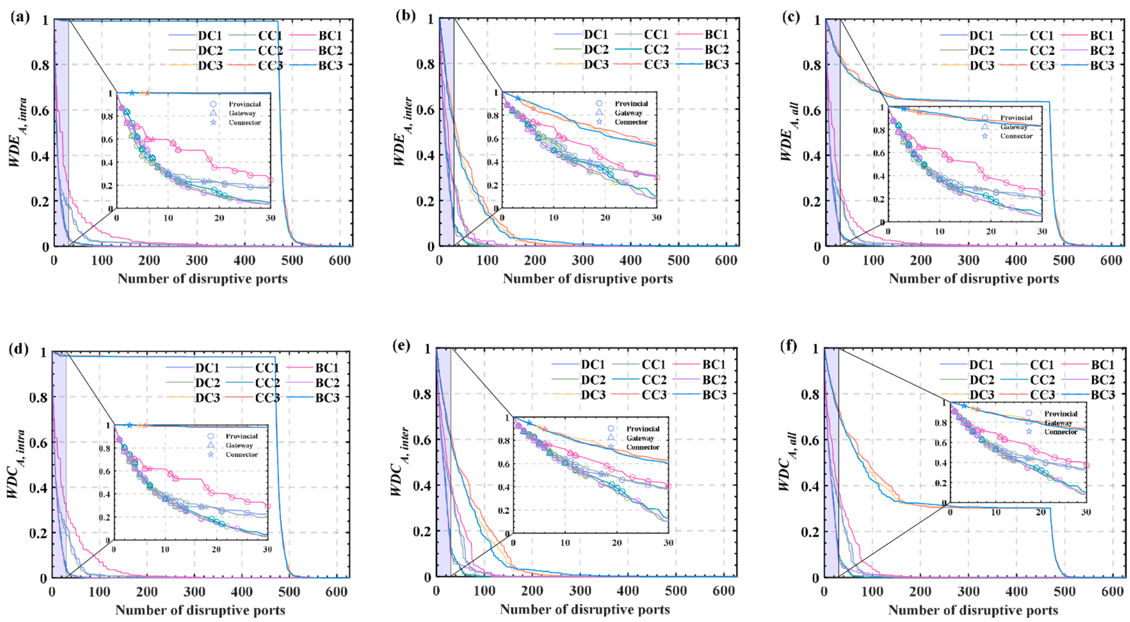

Fig. B1. Variation in $WDEC_A$ for C2 under nine cumulative port disruption scenarios.

Data availability

Data will be made available on request.

References

[1] Liu Q, Yang Y, Ng AKY, Jiang C. An analysis on the resilience of the European port network. Transp Res Part A Policy Pract 2023;175:103778.
[2] Lebedev AO, Lebedeva MP, Butsanets AA. Could the accident of "Ever Given" have been avoided in the Suez Canal? J Phys Conf Ser 2021;2061:12127. IOP Publishing.
[3] Gu B, Liu J. COVID-19 pandemic, port congestion, and air quality: evidence from China. Ocean Coast Manag 2023;235:106497.
[4] Orhan E. The effects of the Russia-Ukraine war on global trade. J Int Trade, Logist Law 2022;8:141–6.
[5] Faturechi R, Miller-Hooks E. Travel time resilience of roadway networks under disaster. Transp Res Part B Methodol 2014;70:47–64.
[6] Sharkey TC, Nurre Pinkley SG, Eisenberg DA, Alderson DL. In search of network resilience: an optimization-based view. Networks 2021;77:225–54.
[7] Nocera F, Contento A, Gardoni P. Risk analysis of supply chains: the role of supporting structures and infrastructure. Reliab Eng Syst Saf 2024;241:109623.
[8] Liu Y, Ma X, Qiao W, Ma L, Han B. A novel methodology to model disruption propagation for resilient maritime transportation systems–a case study of the Arctic maritime transportation system. Reliab Eng Syst Saf 2024;241:109620.
[9] Liu J, Wu J, Gong Y. Maritime supply chain resilience: from concept to practice. Comput Ind Eng 2023;182:109366.
[10] Gu Y, Fu X, Liu Z, Xu X, Chen A. Performance of transportation network under perturbations: reliability, vulnerability, and resilience. Transp Res Part E Logist Transp Rev 2020;133:101809.
[11] Chen J, Liu X, Zhou S, Kang J. Knowledge mapping analysis of resilient shipping network using CiteSpace. Ocean Coast Manag 2023;244:106775.
[12] Su W, Zhang L, Lu J, Zhu J. Crude oil maritime transportation network resilience assessment based on optimal strategies. Transp Res Part D Transp Environ 2025;142:104659.
[13] Xu X, Zhu Y, Xu M, Deng W, Zuo Y. Vulnerability analysis of the global liner shipping network: from static structure to cascading failure dynamics. Ocean Coast Manag 2022;229:106325.
[14] Bai X, Ma Z, Zhou Y. Data-driven static and dynamic resilience assessment of the global liner shipping network. Transp Res Part E Logist Transp Rev 2023;170:103016.
[15] Xu M, Deng W, Zhu Y, Linyuan LÜ. Assessing and improving the structural robustness of global liner shipping system: a motif-based network science approach. Reliab Eng Syst Saf 2023;240:109576.
[16] Wu J, Lu J, Zhang L, Fan H. Spatial heterogeneity among different-sized port communities in directed-weighted global liner shipping network. J Transp Geogr 2024;114:103781.
[17] Xu M, Pan Q, Muscoloni A, Xia H, Cannistraci CV. Modular gateway-ness connectivity and structural core organization in maritime network science. Nat Commun 2020;11:2849.
[18] Yu Y, Liu K, Kong W, Xin X. Time-evolving graph-based approach for multi-ship encounter analysis: insights into ship behavior across different scenario complexity levels. Transp Res Part A Policy Pract 2025;194:104427.
[19] Liu Q, Yang Y, Ke L, Ng AKY. Structures of port connectivity, competition, and shipping networks in Europe. J Transp Geogr 2022;102:103360.
[20] Guo J, Guo S, Lv J. Potential spatial effects of opening Arctic shipping routes on the shipping network of ports between China and Europe. Mar Policy 2022;136:104885.

[21] Xin X, Cao Y, Jarumaneeroj P, Yang Z. Vulnerability assessment of international container shipping networks under national-level restriction policies. Transp Policy 2025.
[22] Poo MC-P, Yang Z, Lau Y. Vulnerability analysis of cruise shipping in ASEAN countries facing COVID-19 pandemic. Ocean Coast Manag 2024;248:106919.
[23] Poo MC-P, Yang Z. Optimising the resilience of shipping networks to climate vulnerability. Marit Policy Manag 2024;51:15–34.
[24] Xu K, Liu J, Li Z. Vulnerability assessments of global liner shipping network based on extended coupled map lattices. Reliab Eng Syst Saf 2025:111306.
[25] Dirzka C, Acciaro M. Global shipping network dynamics during the COVID-19 pandemic's initial phases. J Transp Geogr 2022;99:103265.
[26] Wu D, Yu C, Zhao Y, Guo J. Changes in vulnerability of global container shipping networks before and after the COVID-19 pandemic. J Transp Geogr 2024;114:103783.
[27] Ding C, Li Z, Chen X, Shi X. The evolution and competition patterns of shipping networks under the influence of an Arctic route system. Marit Policy Manag 2022;49:510–27.
[28] Xu Y, Peng P, Claramunt C, Lu F, Yan R. Cascading failure modelling in global container shipping network using mass vessel trajectory data. Reliab Eng Syst Saf 2024;249:110231.
[29] Liu L, Zhang M, Liu C, Yan R, Lang X, Wang H. Shipping map: an innovative method in grid generation of global maritime network for automatic vessel route planning using AIS data. Transp Res Part C Emerg Technol 2025;171:105015.
[30] Jarumaneeroj P, Barnett Lawton J, Svindland M. An evolution of the global container shipping network: port connectivity and trading community structure (2011–2017). Marit Econ Logist 2024;26:283–306.
[31] Wang N, Yuen KF, Gao X, Nie Y. Resilience assessment of global container shipping network via port communities. Transp Res Part D Transp Environ 2025:104649.
[32] Liu M, Liu Y, Wong CWY, Lai K, Tu E. The impacts of geopolitics on global Liquefied Natural Gas (LNG) shipping network: evidence from two geopolitical events. Ocean Coast Manag 2025;267:107706.
[33] Li Z, Luo L, Liu Z. Regional hubs identification in container shipping network based on community connectivity. In: 2023 7th Int Conf Transp Inf Saf. IEEE; 2023. p. 267–74.
[34] He C, Fei X, Cheng Q, Li H, Hu Z, Tang Y. A survey of community detection in complex networks using nonnegative matrix factorization. IEEE Trans Comput Soc Syst 2021;9:440–57.
[35] Kuang D, Yun S, Park H. SymNMF: nonnegative low-rank approximation of a similarity matrix for graph clustering. J Glob Optim 2015;62:545–74.
[36] Chunaev P. Community detection in node-attributed social networks: a survey. Comput Sci Rev 2020;37:100286.
[37] Saeedmanesh M, Geroliminis N. Dynamic clustering and propagation of congestion in heterogeneously congested urban traffic networks. Transp Res Procedia 2017;23:962–79.
[38] Saeedmanesh M, Geroliminis N. Clustering of heterogeneous networks with directional flows based on "Snake" similarities. Transp Res Part B Methodol 2016;91:250–69.
[39] Xin X, Liu K, Loughney S, Wang J, Li H, Yang Z. Graph-based ship traffic partitioning for intelligent maritime surveillance in complex port waters. Expert Syst Appl 2023:120825.
[40] Xin X, Liu K, Loughney S, Wang J, Li H, Ekere N, et al. Multi-Scale Collision Risk Estimation for Maritime Traffic in Complex Port Waters. Reliab Eng Syst Saf 2023:109554.
[41] Xin X, Liu K, Li H, Yang Z. Maritime traffic partitioning: an adaptive semi-supervised spectral regularization approach for leveraging multi-graph evolutionary traffic interactions. Transp Res Part C Emerg Technol 2024;164:104670.
[42] Wang F, Tian J, Ling J, Chen Z, Xu Z. A multi-stage resilience analysis framework of critical infrastructure systems based on component importance measures. Reliab Eng Syst Saf 2025;256:110720.
[43] He Y, Zio E, Yang Z, Xiang Q, Fan L, He Q, et al. A systematic resilience assessment framework for multi-state systems based on physics-informed neural network. Reliab Eng Syst Saf 2025:110866.
[44] Gonçalves L, Ribeiro PJG. Resilience of urban transportation systems. Concept, characteristics, and methods. J Transp Geogr 2020;85:102727.
[45] Dui H, Zheng X, Wu S. Resilience analysis of maritime transportation systems based on importance measures. Reliab Eng Syst Saf 2021;209:107461.
[46] Qin Y, Guo J, Liang M, Feng T. Resilience characteristics of port nodes from the perspective of shipping network: empirical evidence from China. Ocean Coast Manag 2023;237:106531.
[47] Asadabadi A, Miller-Hooks E. Maritime port network resiliency and reliability through co-opetition. Transp Res Part E Logist Transp Rev 2020;137:101916.
[48] Viljoen NM, Joubert JW. The vulnerability of the global container shipping network to targeted link disruption. Phys A Stat Mech Its Appl 2016;462:396–409.
[49] Liu H, Tian Z, Huang A, Yang Z. Analysis of vulnerabilities in maritime supply chains. Reliab Eng Syst Saf 2018;169:475–84.
[50] Cao Y, Xin X, Jarumaneeroj P, Li H, Feng Y, Wang J, et al. Data-driven resilience analysis of the global container shipping network against two cascading failures. Transp Res Part E Logist Transp Rev 2025;193:103857.
[51] Ghosh P, De M. Effectiveness of network centrality for improving distribution system resilience by hardening. In: 2022 IEEE Glob Conf Comput Power Commun Technol. IEEE; 2022. p. 1–6.
[52] Zhou Y, Kundu T, Qin W, Goh M, Sheu J-B. Vulnerability of the worldwide air transportation network to global catastrophes such as COVID-19. Transp Res Part E Logist Transp Rev 2021;154:102469.
[53] Calatayud A, Mangan J, Palacin R. Vulnerability of international freight flows to shipping network disruptions: a multiplex network perspective. Transp Res Part E Logist Transp Rev 2017;108:195–208.
[54] Ding C, He X, Simon HD. On the equivalence of nonnegative matrix factorization and spectral clustering. In: Proc 2005 SIAM Int Conf Data Min, SIAM; 2005. p. 606–10.
[55] Ma X, Dong D. Evolutionary nonnegative matrix factorization algorithms for community detection in dynamic networks. IEEE Trans Knowl Data Eng 2017;29:1045–58.
[56] Estrada E. The structure of complex networks: theory and applications. American Chemical Society; 2012.
[57] Bharti D, De M. A centrality index based approach for selection of optimal location of static reactive power compensator. Electr Power Components Syst 2018;46:886–99.
[58] Li S, Zhou Y, Kundu T, Zhang F. Impact of entry restriction policies on international air transport connectivity during COVID-19 pandemic. Transp Res Part E Logist Transp Rev 2021;152:102411.
[59] Wang K, Jiang C, Ng AKY, Zhu Z. Air and rail connectivity patterns of major city clusters in China. Transp Res Part A Policy Pract 2020;139:35–53.
[60] Jarumaneeroj P, Ramudhin A, Barnett Lawton J. A connectivity-based approach to evaluating port importance in the global container shipping network. Marit Econ Logist 2023;25:602–22.
[61] Zhang J, Xin X, Liao Z, Dubey R, Nguyen TT, Li N, et al. Analysis of the ripple effects of disruptions on multimodal container terminals operations: a System Dynamics approach. Transp Res Part E Logist Transp Rev 2025;202:104264.
[62] Xin X, Liu K, Yu Y, Yang Z. Developing robust traffic navigation scenarios for autonomous ship testing: an integrated approach to scenario extraction, characterization, and sampling in complex waters. Transp Res Part C Emerg Technol 2025;178:105246.
[63] Xin X., Liu K., Liu J., Wang W., Yang Z. Modeling, Evaluation, and Mitigation of Maritime Traffic Complexity in Complex Waters. IEEE Trans Intell Transp Syst 2025.